Jefferson Lab

Theory Seminar

Quantum Simulation of Phase Transitions

Fanyi Zhao

Supported by Graduate fellowship in quantum information science

Bhaumik Institute for Theoretical Physics,
University of California, Los Angeles (UCLA)

arXiv:**2112.03944**
arXiv:**2210.03062**

November 28th 2022

Sketch of the QCD phase diagram

Temperature

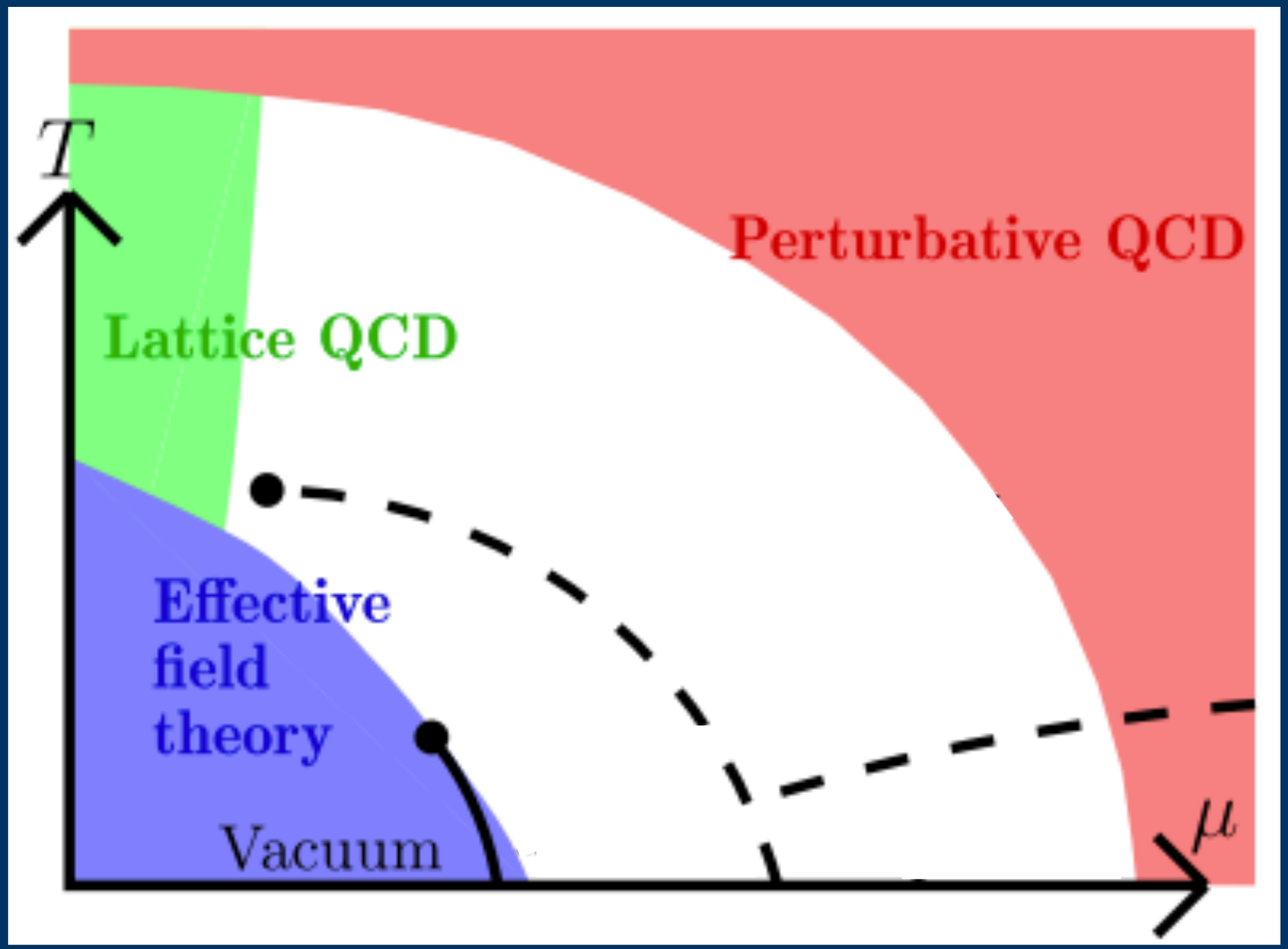

Baryon Chemical Potential

[Matti Järvinen, 2022]

Phase diagram: division of the T-μ plane into regions based on the qualitative physical properties of strongly interacting matter

My primary interest in research can be cast into two categories: perturbative and non-perturbative QCD.

Sketch of the QCD phase diagram

Temperature

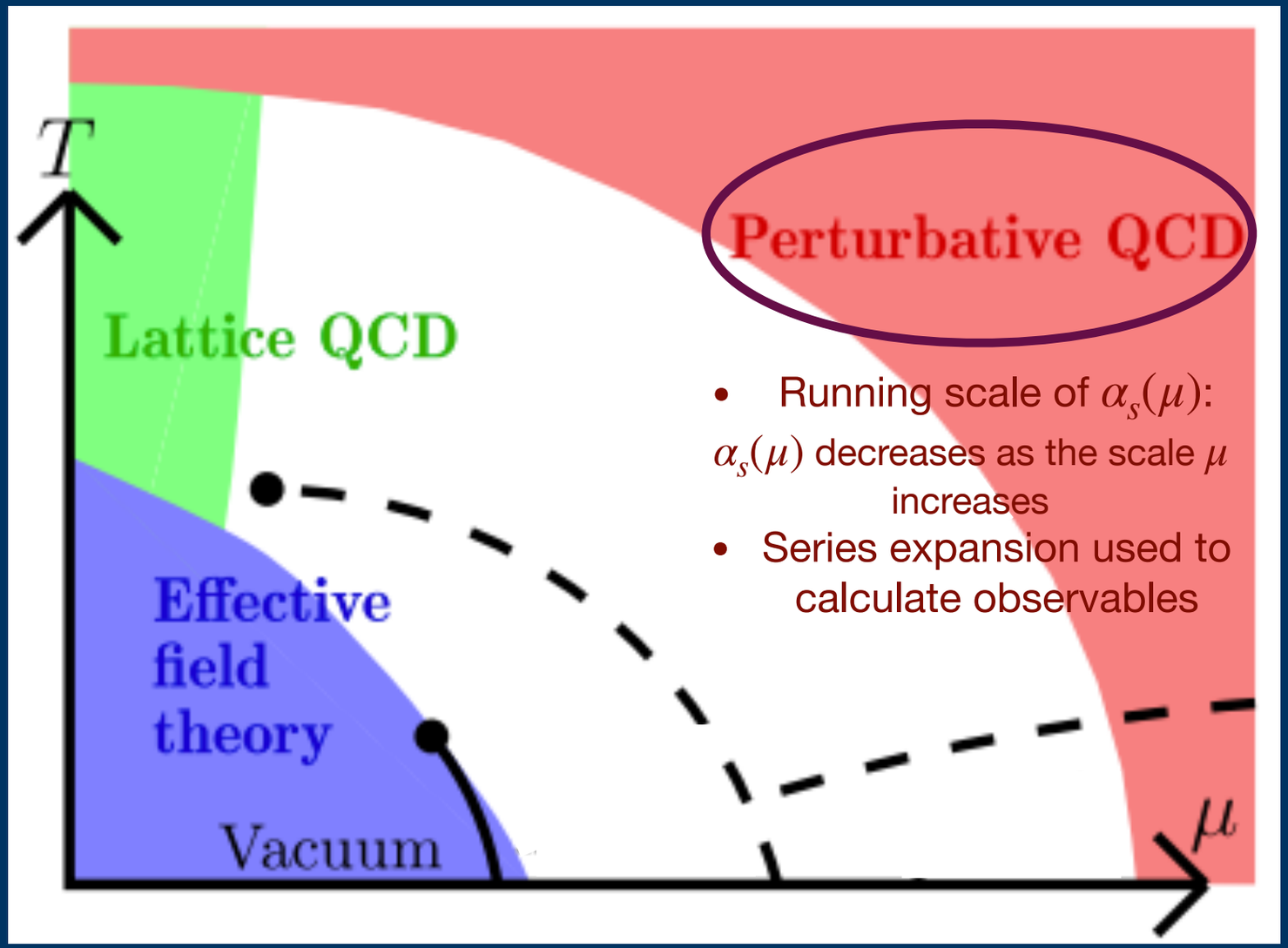

- Running scale of $\alpha_s(\mu)$:

$\alpha_s(\mu)$ decreases as the scale μ increases

- Series expansion used to calculate observables

- TMDs
- Jets

Baryon Chemical Potential

[Matti Järvinen, 2022]

Phase diagram: division of the T-μ plane into regions based on the qualitative physical properties of strongly interacting matter

My primary interest in research can be cast into two categories: perturbative and non-perturbative QCD.

Transverse Momentum Dependent distributions (**TMDs**): 3D imaging in momentum space[A. Bacchetta et al., 2017, D. Callos et al., 2020, P. Barry et al., 2022, etc.]

- Both longitudinal and transverse motion
- What are the quantum correlations between the motion of the quarks/gluons, their spin and the spin of the proton? (TMD PDFs)
- Similarly precision information on hadronization (TMD FFs)

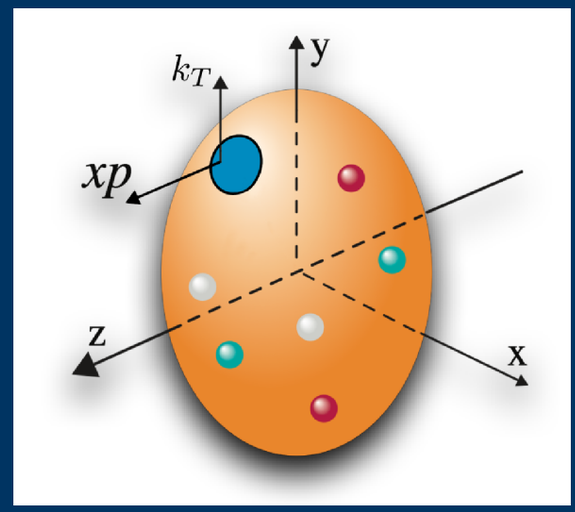

- **TMDs**
- Jets

Transverse Momentum Dependent distributions (**TMDs**): 3D imaging in momentum space[A. Bacchetta et al., 2017, D. Callos et al., 2020, P. Barry et al., 2022, etc.]

- Both longitudinal and transverse motion
- What are the quantum correlations between the motion of the quarks/gluons, their spin and the spin of the proton? (TMD PDFs)
- Similarly precision information on hadronization (TMD FFs)

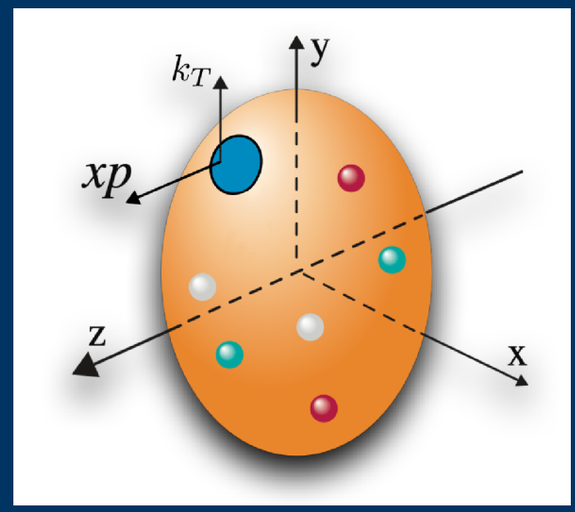

Jets for 3D imaging

- Jets production: correlated with TMD PDFs, without fragmentation function[HERA, PRL 2021, M.Arratia et al., 2020]
- Jet substructure: One can further measure distribution of hadrons inside the jet (TMD JFFs)[Z. Kang et al., 2020, M.Arratia et al., 2020, Z. Kang et al., 2021, Z. Kang et al., 2022]

Novel probes for 3D structure of the nucleon and nuclei (encoded in TMD PDFs, FFs)

- **TMDs**
- **Jets**

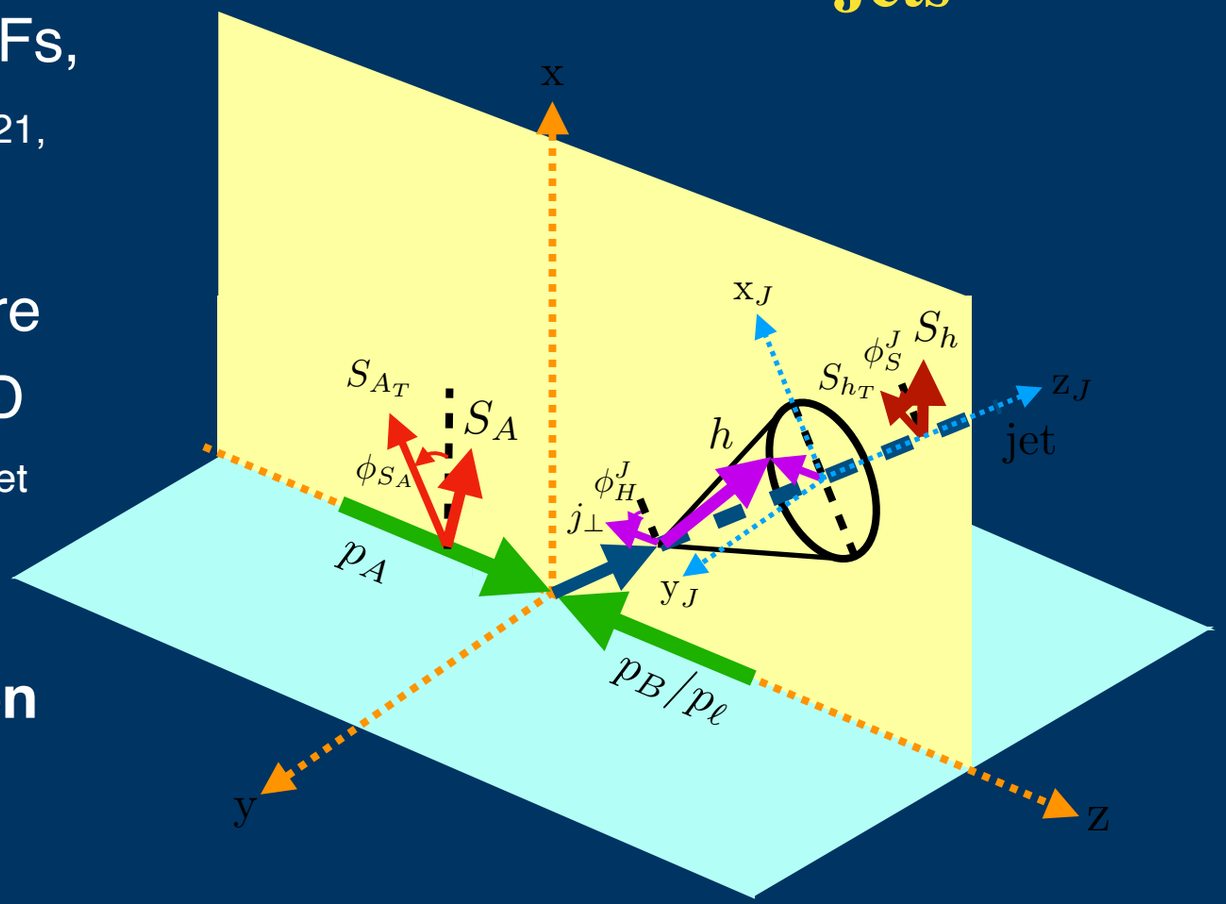

Sketch of the QCD phase diagram

Temperature

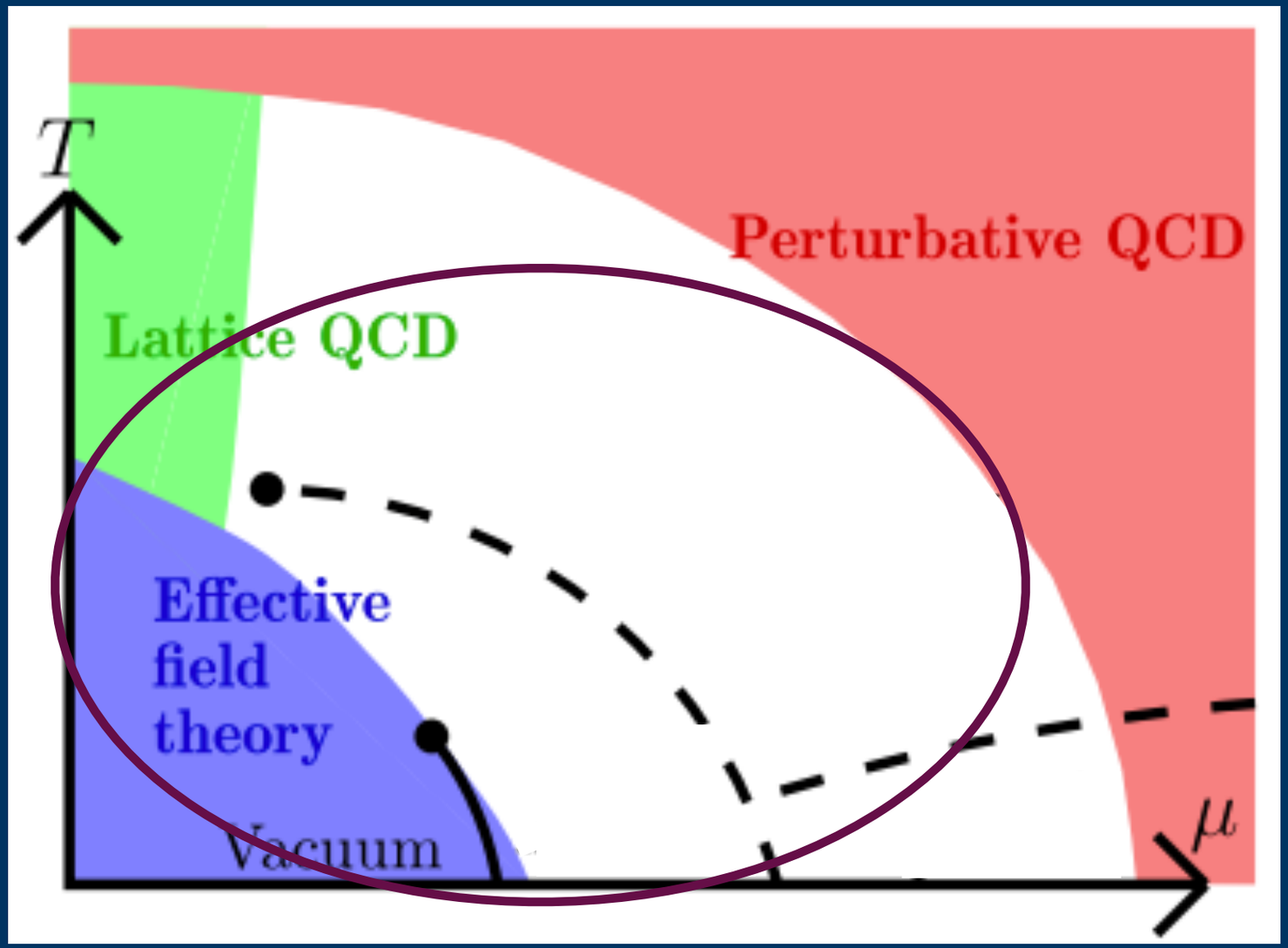

Baryon Chemical Potential

[Matti Järvinen, 2022]

Non-perturbative QCD:
Quantum computing for QCD

Research Interests

Non-perturbative QCD:

Quantum computing for QCD

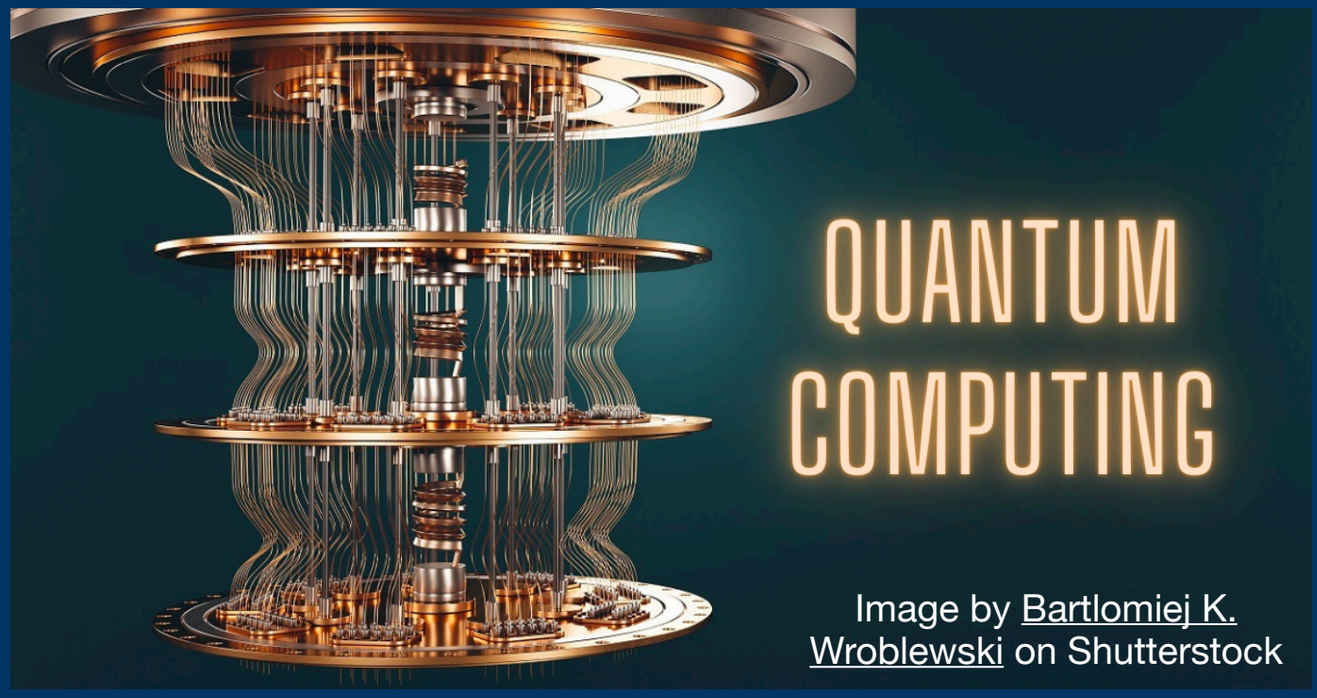

Image by Bartlomiej K. Wroblewski on Shutterstock

Motivation:

- Quantum computing is a relatively new and upcoming technology that uses the principles of quantum physics to solve complex problems.
- If powerful and reliable quantum computers become reality in the upcoming years, can we begin simulating matter and its dynamics from first-principles using such a new computing tool?

Quantum Simulation of Chiral Phase Transitions

arXiv:**2112.03944**, JHEP 08 (2022), 209

In collaboration with A. M. Czajka, Z.-B. Kang, H. Ma

A. M. Czajka

UCLA

↓

UCLA

Z.-B. Kang

H. Ma

UCLA

↓

MIT

Studying chirality imbalance with quantum algorithms

arXiv:**2210.03062**

In collaboration with A. M. Czajka, Z.-B. Kang, Y. Tee

A. M. Czajka

Z.-B. Kang

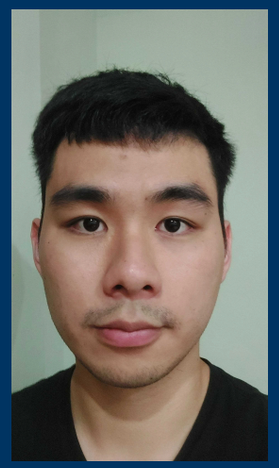

Y. Tee

UCLA

We apply the Quantum Imaginary Time Evolution (QITE) algorithm to simulate the chiral phase transition in 1+1-dimensional Nambu-Jona-Lasinio (NJL) model

Quantum Simulation of Phase Transitions

- Background

  Quantum Computing, NJL model and the chiral magnetic effect (CME)
- Nambu-Jona-Lasinio (NJL) model
- Quantum Imaginary Time Evolution (QITE)
- Results
- Summary

Why QC for QCD?

From Quantum Computing:

- Progress in quantum computing
- Accessibility to quantum simulators and devices:
  1. Enter through cloud services
  2. Build quantum circuits using single-qubit gates and CNOT gate
  3. Obtain outputs from simulators and hardwares

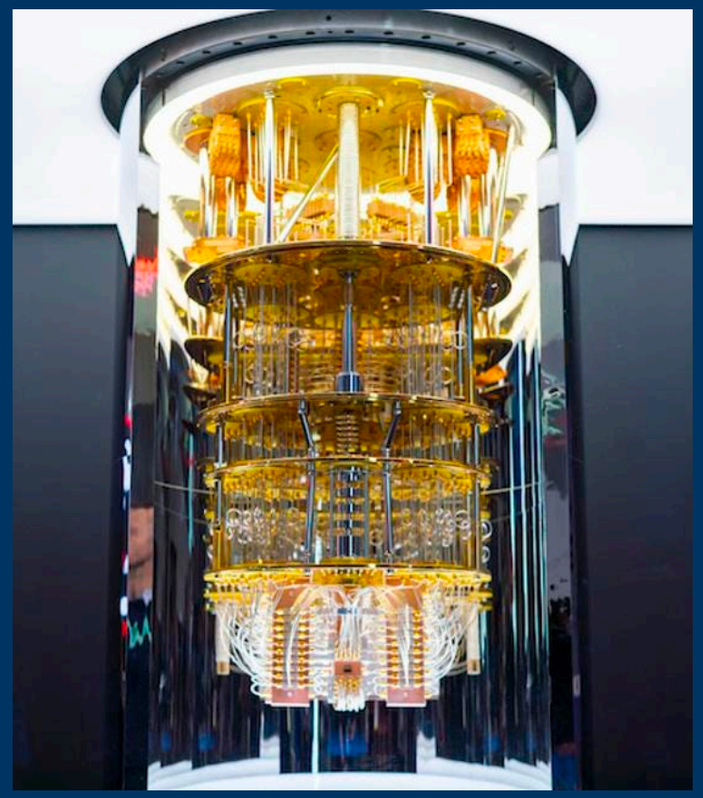

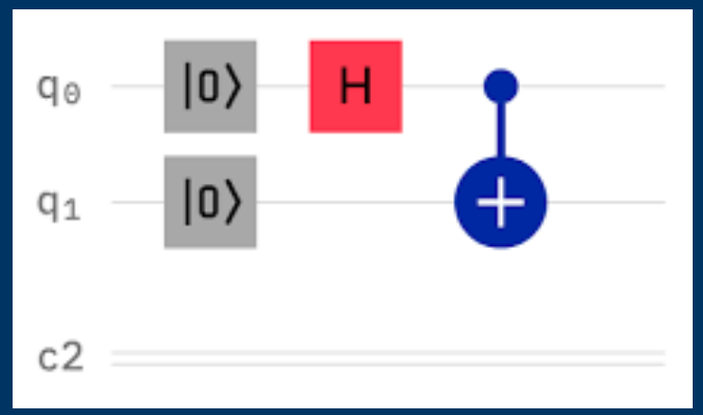

Images by IBMQ

Why QC for QCD?

From QCD:

- Problems in QCD[Joseph I. Kapusta et al., 2006]:
  - Finite density QCD (sign problem)[A. M. Czajka et al,. 2021]
  - Real-time evolution for QCD[Dmitri Kharzeev et al., 2020]
  - Hard interaction, parton shower[Khadeejah Bepari et al. 2020]

Image by IBMQ

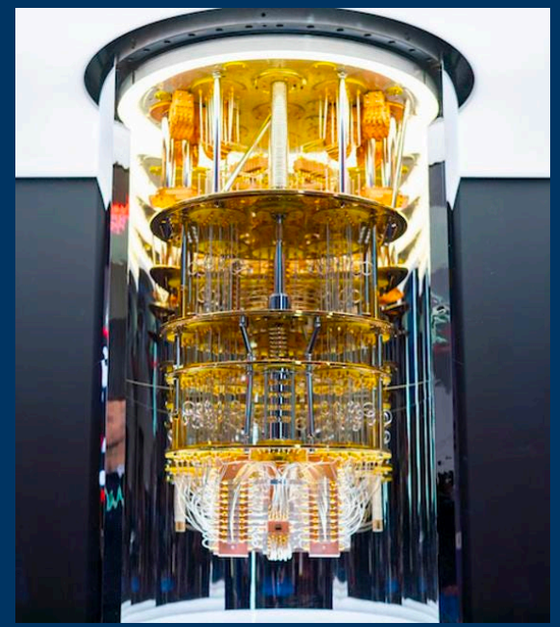

Why QC for QCD?

From QCD:

- Problems in QCD[Joseph I. Kapusta et al., 2006]:
  - Finite density QCD (sign problem)[A. M. Czajka et al,. 2021]
  - Real-time evolution for QCD[Dmitri Kharzeev et al., 2020]
  - Hard interaction, parton shower[Khadeejah Bepari et al. 2020]

Image by IBMQ

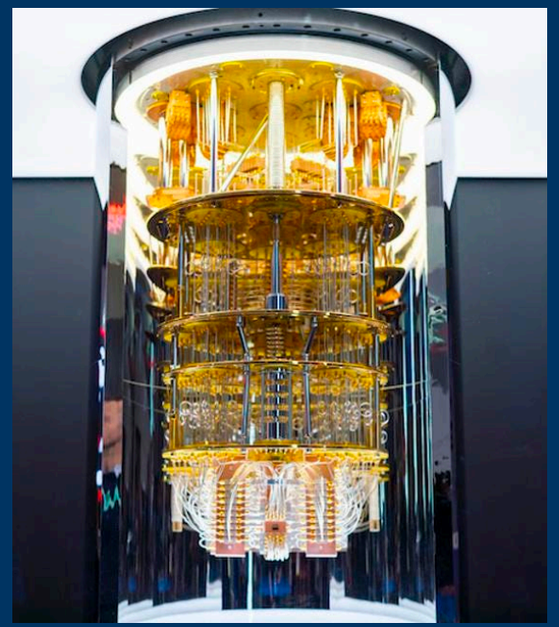

- A quantum computer can do better than a classical one for QCD in[John Preskill, 2018]
  - Study particle collisions at strong coupling
  - Explore structure and properties of strongly interacting nuclear matter

Why QC for QCD?

From QCD:

- Problems in QCD[Joseph I. Kapusta et al., 2006]:
  - Finite density QCD (sign problem)**[A. M. Czajka et al,. 2021]**
  - Real-time evolution for QCD[Dmitri Kharzeev et al., 2020]
  - Hard interaction, parton shower[Khadeejah Bepari et al. 2020]

Image by IBMQ

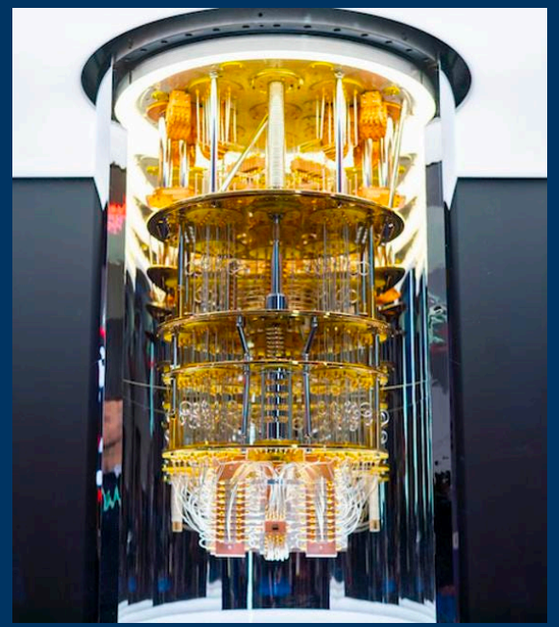

- A quantum computer can do better than a classical one for QCD in[John Preskill, 2018]
  - Study particle collisions at strong coupling
  - Explore structure and properties of strongly interacting nuclear matter

⇒ **We will show how a quantum algorithm helps in studying QCD chiral phase transition**

- To investigate the structure of the QCD chiral phase diagram, calculations are typically carried out in lattice QCD.

- However, the utility of this traditional approach is limited by the fermion sign problem.

- At $\mu \neq 0$, one finds the complex conjugate of the Fermion determinant $[\det M(\mu)]^* = [\det M(-\mu^*)]$ with $M^\dagger(\mu) = \gamma_5 M(-\mu^*)\gamma_5$, the Euclidean QCD action S is no longer constrained to be real,

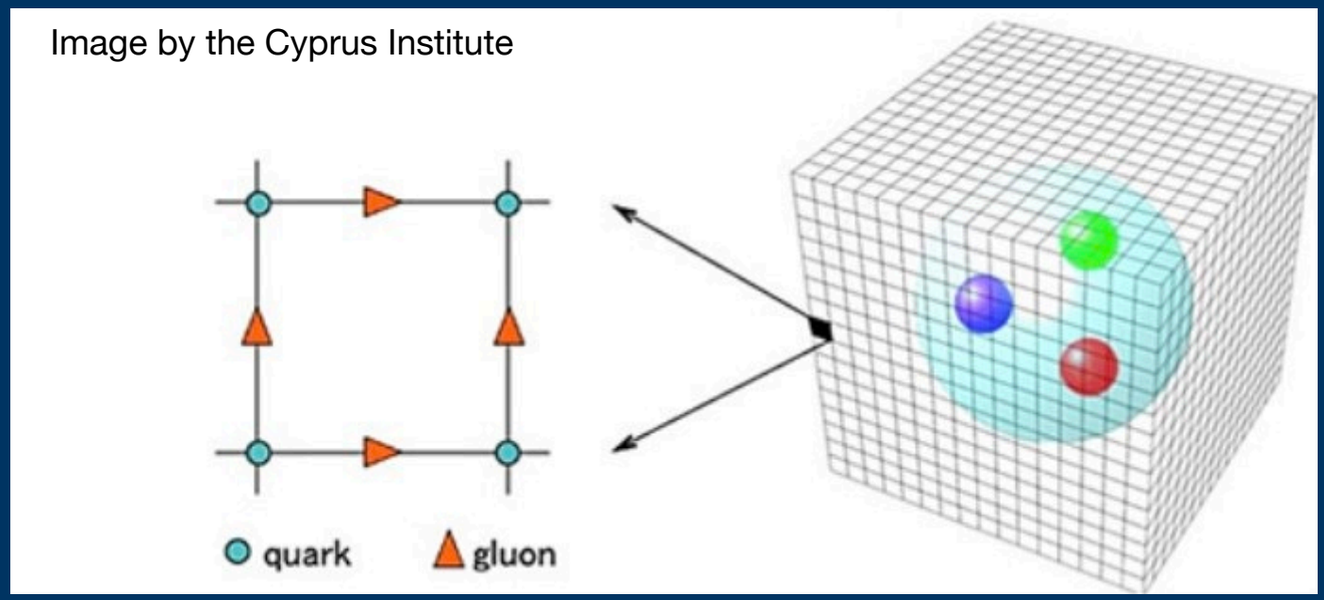

$$\mathscr{L} = \bar{\psi}(i\gamma_\mu \partial^\mu - m + \mu\gamma_0)\psi - \mathscr{V}$$

$$S = \int_0^\beta d\tau \int dx \bar{\psi} \left[i\gamma_\mu \partial^\mu - m + \mu\gamma_0 \right] \psi = \int d^2x \bar{\psi} M \psi$$

- With the QCD Lagrangian and action given above, the Boltzmann factor $\exp[-S]$ can no longer be used as a weight for a Monte Carlo evaluation of thermal expectation values.
- Though many attempts were developed to overcome or avoid the sign problem, results are only consistent at small μ $(\mu/T < 1)$, but not reliable at larger μ

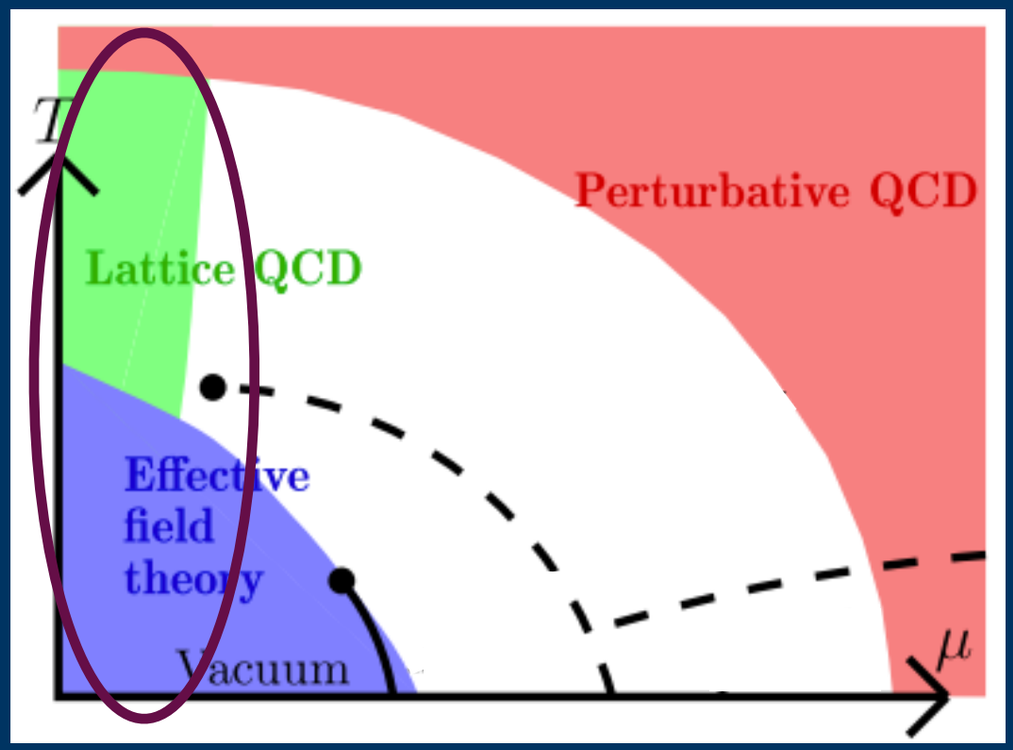

QCD Phase diagram

- Complex phase structure of strongly interacting matter in theory

The “current conjecture” for the QCD phase diagram

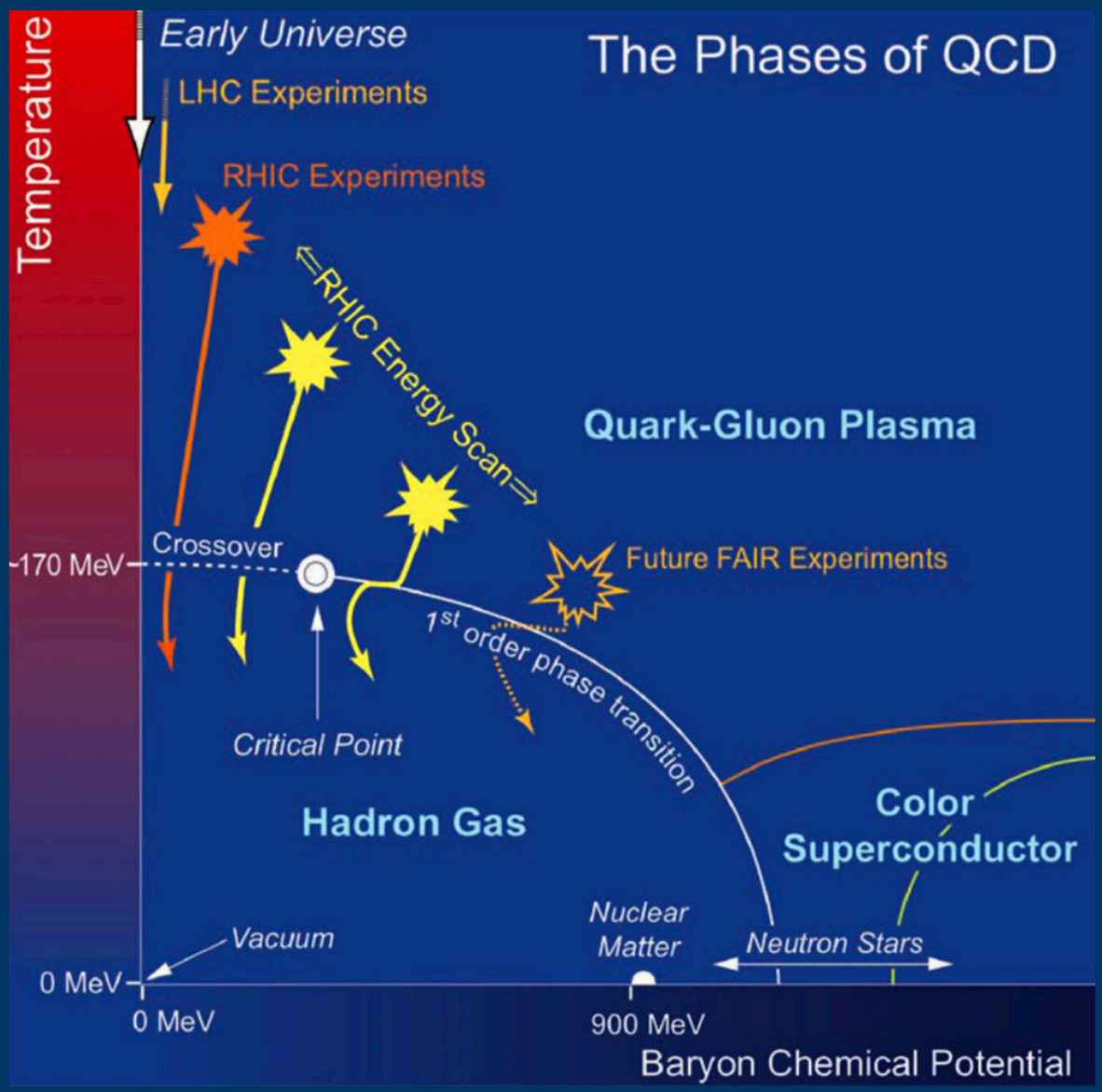

Phase diagram: division of the T-μ plane into regions based on the qualitative physical properties of strongly interacting matter

QCD Phase diagram

- Complex phase structure of strongly interacting matter in theory
- In experiment (e.g. Beam Energy Scan at RHIC), one of the most accessible ways to characterize properties of QCD

The “current conjecture” for the QCD phase diagram

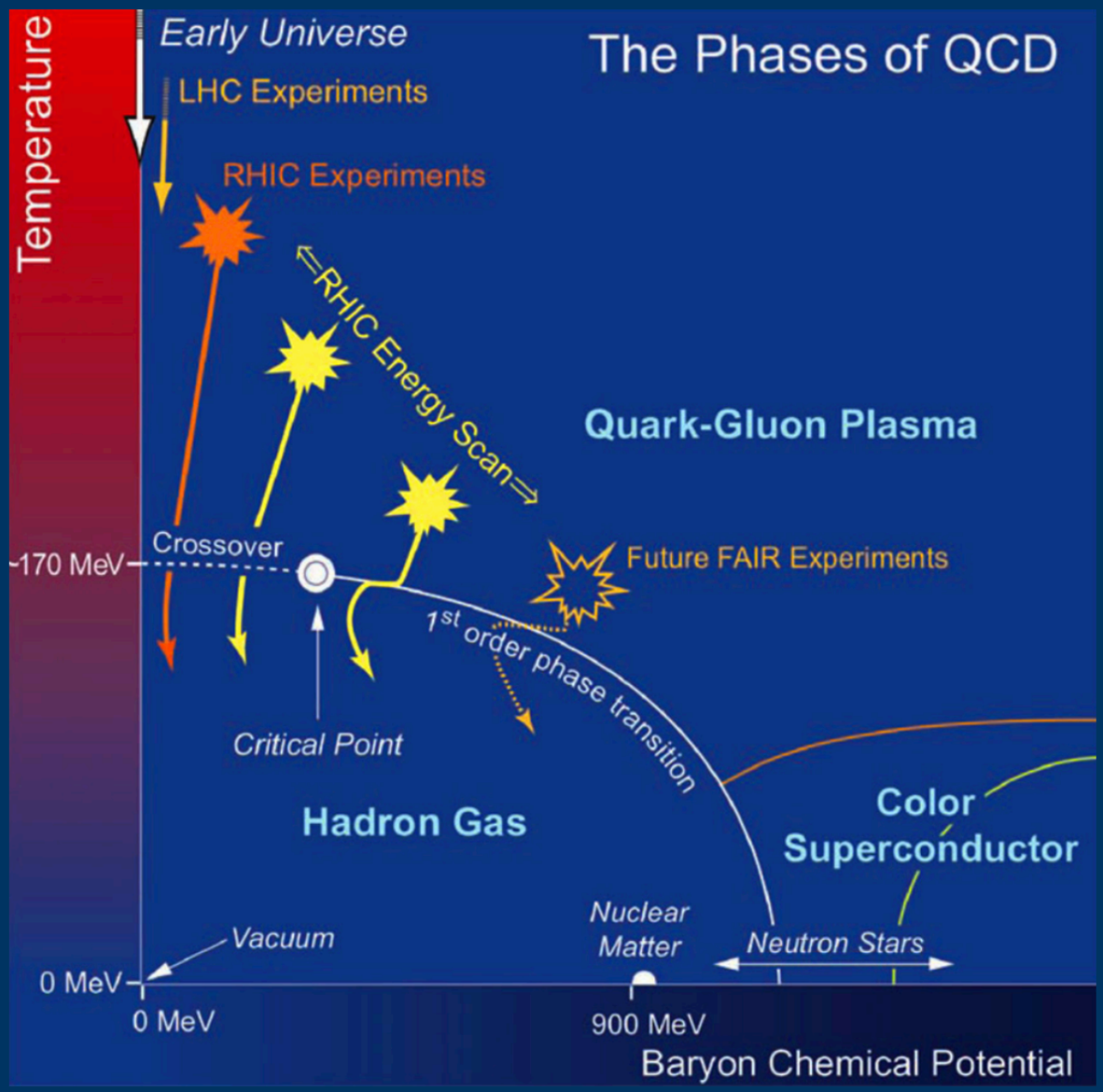

Phase diagram: division of the T-μ plane into regions based on the qualitative physical properties of strongly interacting matter

Chiral Magnetic Effect (CME)

- It is of great interest to study how non-perturbative features of QCD are affected by thermal excitations in a strong magnetic field B at high temperatures[D. Kharzeev and A. Zhitnitsky, 2007], and by baryon-rich matter at finite chemical potentials μ and μ_5[D. Kharzeev, et al., 2015].

In non-central collisions of heavy-ion collisions, a strong magnetic field is created $\perp \Psi_R$ [Dmitri Kharzeev, 2013]

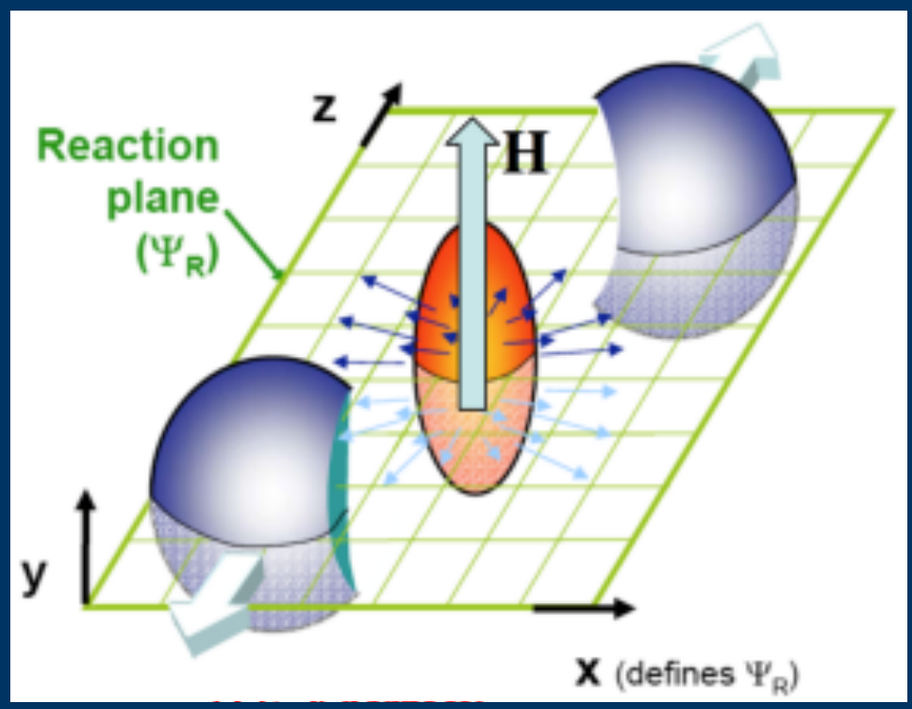

Chiral Magnetic Effect (CME)

- It is of great interest to study how non-perturbative features of QCD are affected by thermal excitations in a strong magnetic field B at high temperatures[D. Kharzeev and A. Zhitnitsky, 2007], and by baryon-rich matter at finite chemical potentials μ and μ_5[D. Kharzeev, et al., 2015].

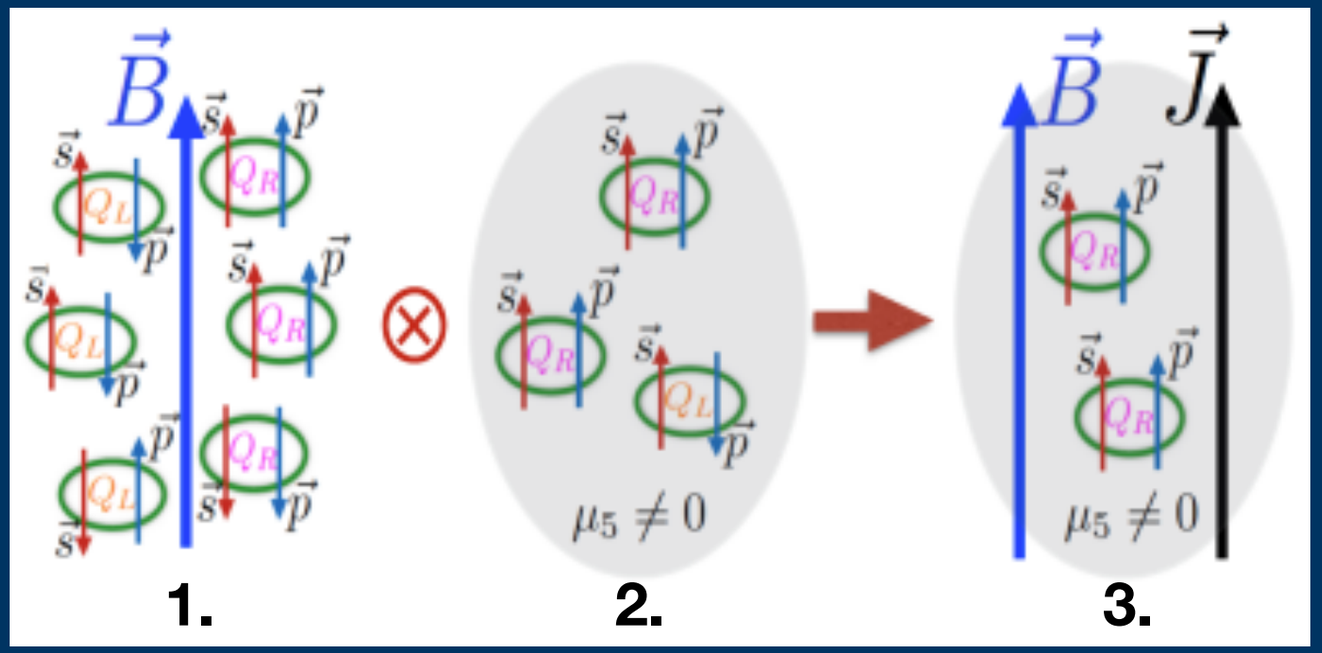

1.
- Quarks' spins preferably aligned along the $\vec{B}$ field direction
- Quarks with specific chirality have their momentum $\vec{p}$ direction correlated with spin $\vec{s}$ orientation

Chiral Magnetic Effect (CME)

- It is of great interest to study how non-perturbative features of QCD are affected by thermal excitations in a strong magnetic field B at high temperatures[D. Kharzeev and A. Zhitnitsky, 2007], and by baryon-rich matter at finite chemical potentials μ and μ_5[D. Kharzeev, et al., 2015].

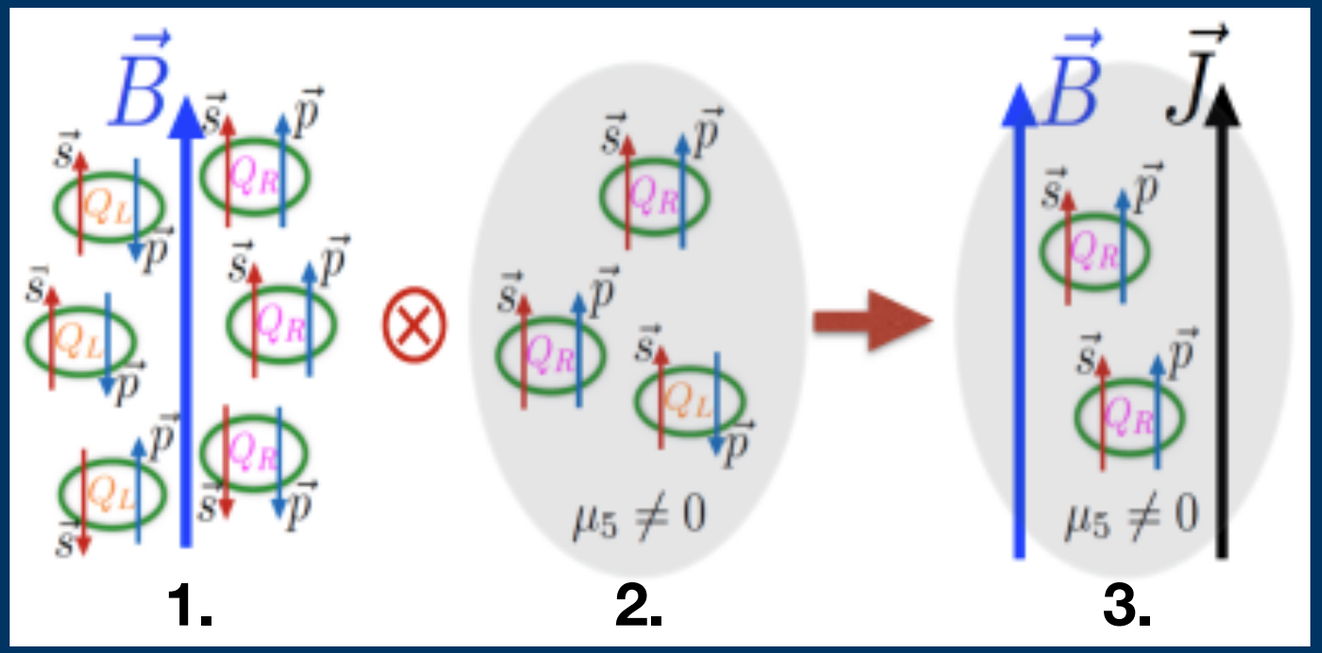

2.

- In the presence of chirality imbalance $\mu_5 \neq 0$, there will be a net correlation between average spin and momentum

Chiral Magnetic Effect (CME)

- It is of great interest to study how non-perturbative features of QCD are affected by thermal excitations in a strong magnetic field B at high temperatures[D. Kharzeev and A. Zhitnitsky, 2007], and by baryon-rich matter at finite chemical potentials μ and μ_5[D. Kharzeev, et al., 2015].

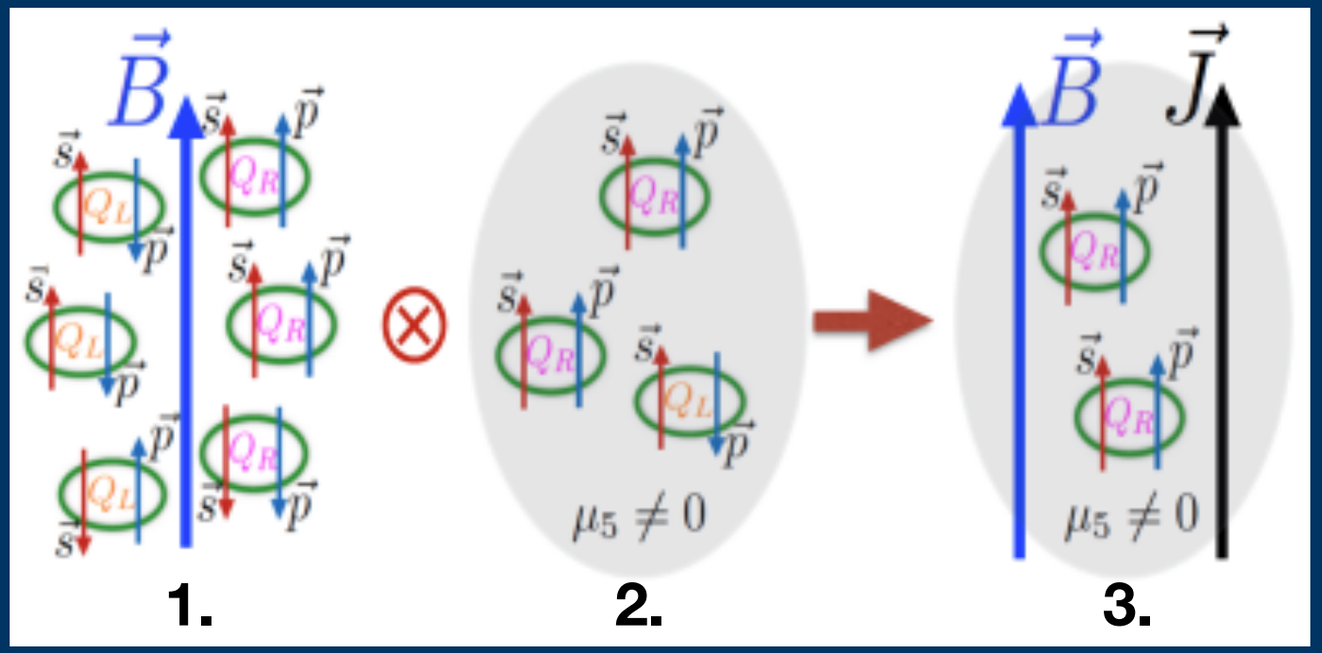

3. • $\mu_5 > 0$ leads to an electric current along the magnetic field

Chiral Magnetic Effect (CME)

- In the presence of a magnetic field, an imbalance is produced between right- and left-handed quarks, namely the so-called Chiral Magnetic Effect (CME)[D. Kharzeev and A. Zhitnitsky, 2007].

[D. Kharzeev, et al., 2015]

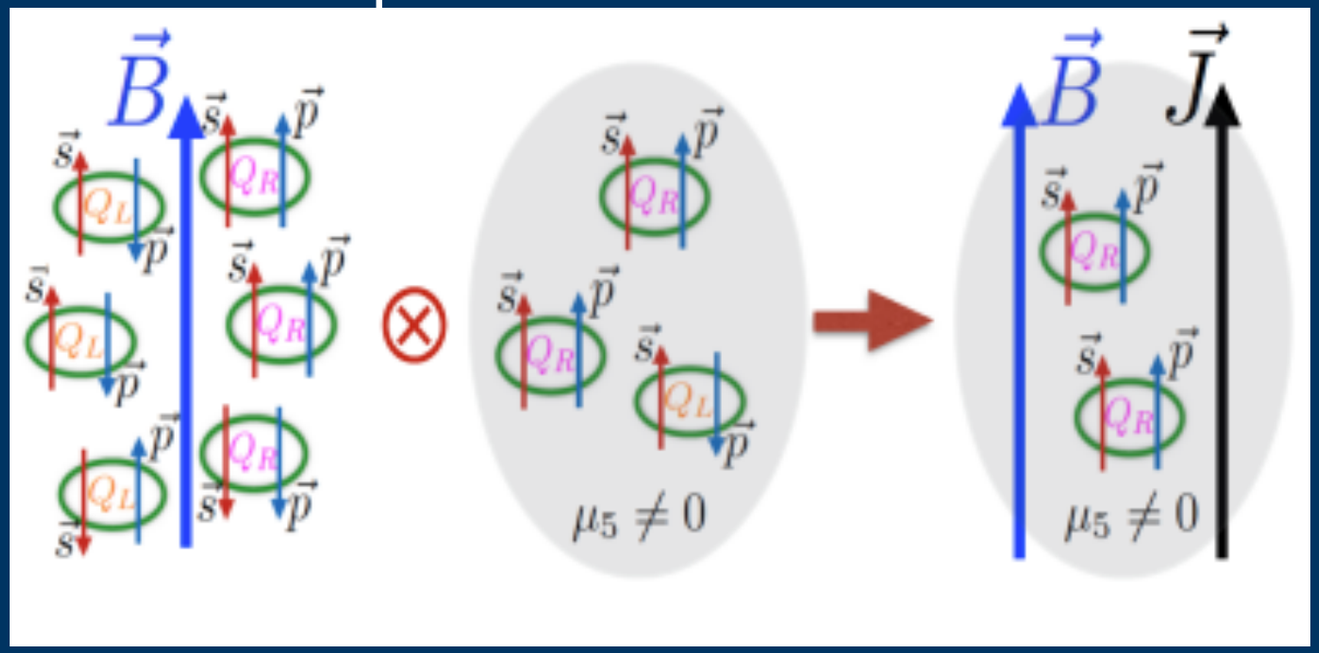

- By introducing a finite chiral chemical potential μ_5 that imitates the effects of the topological charge changing transitions, one can study the QCD phase diagram.

Why Nambu-Jona-Lasinio model?

- The NJL model[Y. Nambu and G. Jona-Lasinio, 1961] is an effective model for QCD
  - A convenient and practical tool to study the QCD chiral phase transition
  - Simulating QCD is not possible at the moment, we work with a simple model

$$\mathscr{L} = \bar{\psi}(i\gamma_\mu \partial^\mu - m)\psi + g(\bar{\psi}\psi)^2$$

- A renormalizable and asymptotically free (1+1)-dimensional theory
- Comprised of fermions interacting via four-fermion contact interaction.

Why Nambu-Jona-Lasinio model?

- The NJL model[Y. Nambu and G. Jona-Lasinio, 1961] is an effective model for QCD
  - A convenient and practical tool to study the QCD chiral phase transition
  - Simulating QCD is not possible at the moment, we work with a simple model

★ We study the chiral phase transition of NJL model with non-zero chemical potential μ (the imbalance between matter and antimatter) and μ_5 (chirality imbalance)

$$\mathscr{L} = \bar{\psi}(i\gamma_\mu \partial^\mu - m)\psi + g(\bar{\psi}\psi)^2$$

$$\Downarrow$$

$$\mathscr{L} = \bar{\psi}(i\gamma_\mu \partial^\mu - m)\psi + g(\bar{\psi}\psi)^2 + \mu\bar{\psi}\gamma_0\psi + \mu_5\bar{\psi}\gamma_0\gamma_5\psi$$

⇒ amenable to analytical calculations at finite temperature and chemical potential

Analytical calculation

of the chiral condensate in (1+1) dimensional NJL model:

$$\mathscr{L} = \bar{\psi}(i\gamma_\mu \partial^\mu - m)\psi + g(\bar{\psi}\psi)^2 + \mu\bar{\psi}\gamma_0\psi + \mu_5\bar{\psi}\gamma_0\gamma_5\psi$$

- In (1+1) dimensions, the gamma matrices are given by
  $\gamma_0 = Z,\ \gamma_1 = -iY,\ \gamma_5 = \gamma_0\gamma_1 = -X$

- Mean field approximation: $\bar{\psi}\psi = \langle\bar{\psi}\psi\rangle + \sigma$, where $\langle\bar{\psi}\psi\rangle$ is the thermal average and σ is a real scalar field fluctuations, assumed to be small, i.e.
  $|\sigma/\langle\bar{\psi}\psi\rangle| \ll 1$

Analytical calculation

of the chiral condensate in (1+1) dimensional NJL model:

$$\mathscr{L} = \bar{\psi}(i\gamma_\mu \partial^\mu - m)\psi + g(\bar{\psi}\psi)^2 + \mu\bar{\psi}\gamma_0\psi + \mu_5\bar{\psi}\gamma_0\gamma_5\psi$$

- In (1+1) dimensions, the gamma matrices are given by
  $\gamma_0 = Z,\ \gamma_1 = -iY,\ \gamma_5 = \gamma_0\gamma_1 = -X$
- Mean field approximation: $\bar{\psi}\psi = \langle\bar{\psi}\psi\rangle + \sigma$, where $\langle\bar{\psi}\psi\rangle$ is the thermal average and σ is a real scalar field fluctuations, assumed to be small, i.e.
  $|\sigma/\langle\bar{\psi}\psi\rangle| \ll 1$

$$\Rightarrow \quad \mathscr{L} = \bar{\psi}(i\gamma_\mu\partial^\mu - m + 2g\langle\bar{\psi}\psi\rangle + \mu\gamma_0)\psi - g\langle\bar{\psi}\psi\rangle^2 + \mathcal{O}(\sigma^2)$$

$$\approx \boxed{\bar{\psi}(i\gamma_\mu\partial^\mu - M + \mu\gamma_0)\psi} - \mathscr{V}$$

Free Dirac fermion at μ with effective mass M

Effective mass $M = m - 2g\langle\bar{\psi}\psi\rangle$ and potential $\mathscr{V} = \dfrac{(M-m)^2}{4g}$

Analytical calculation

of the chiral condensate in (1+1) dimensional NJL model:

$$\mathscr{L} = \bar{\psi}(i\gamma_\mu \partial^\mu - m)\psi + g(\bar{\psi}\psi)^2 + \mu\bar{\psi}\gamma_0\psi + \mu_5\bar{\psi}\gamma_0\gamma_5\psi$$

★ The Grand Canonical Potential Ω:

$$\Omega(\mu, \mu_5, T; M) = \mathscr{V} - \frac{2}{\pi}\sum_s \int_0^\infty \left[T\ln(1 + e^{-\beta(\omega_{k,s}+\mu)}) + T\ln(1 + e^{-\beta(\omega_{k,s}-\mu)}) + \omega_{k,s}\right] dk\,.$$

$$\mathscr{V} = (M-m)^2/4g \qquad \omega_{k,s} = \sqrt{(k + s\mu_5)^2 + M^2} \qquad s = \pm 1$$

- For comparison with numerical results with the lattice spacing a, the natural momentum cutoff is $\Lambda = \pi/a$
- Next, we are able to write down the Grand Canonical Potential Ω and numerically solving the **gap equation** $\dfrac{\partial\Omega(\mu, \mu_5, T; M)}{\partial M} = 0.$

Analytical calculation

of the chiral condensate in (1+1) dimensional NJL model:

- **The gap equation** $\dfrac{\partial\Omega(\mu,\mu_5,T;M)}{\partial M}=0.$

- (1+1)-d NJL model: One can easily carry out the numerical integral on a classical computer **without worrying about the sign problem** with Monte Carlo methods.

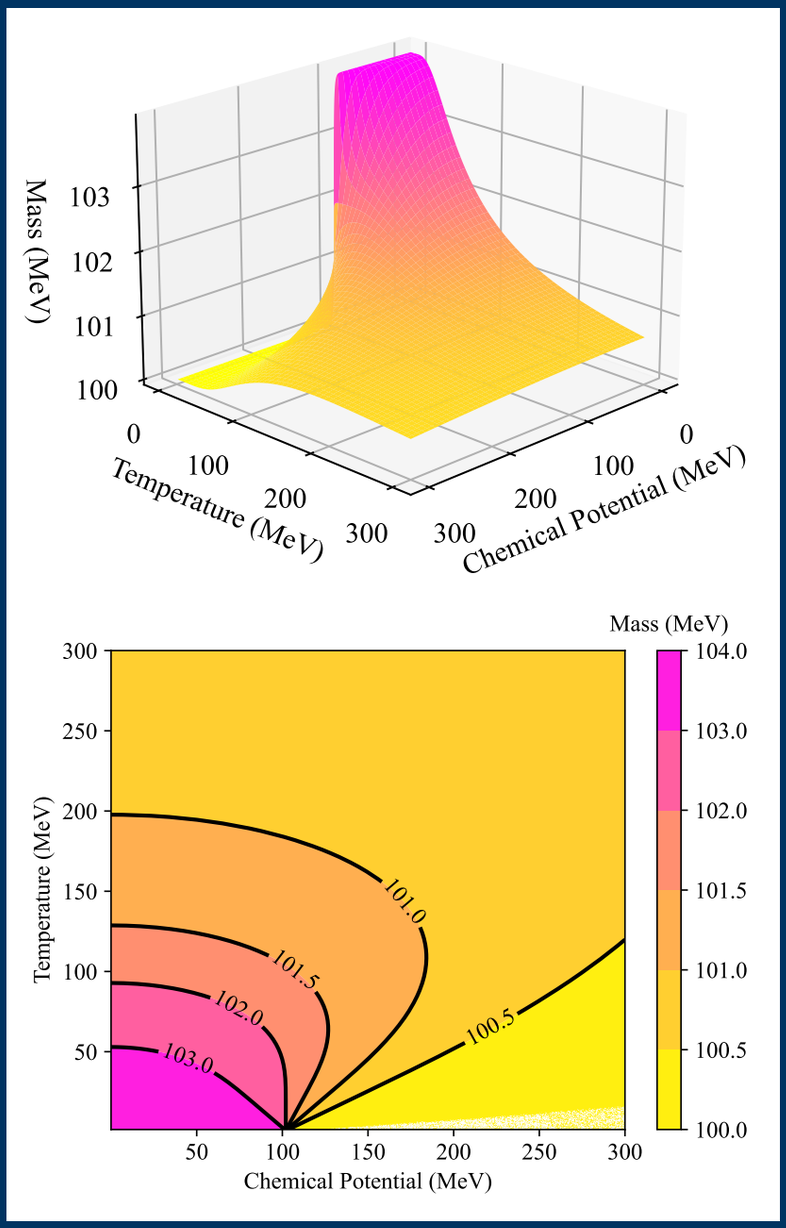

Analytical calculation

of the chiral condensate in (1+1) dimensional NJL model:

- **The gap equation** $\dfrac{\partial\Omega(\mu,\mu_5,T;M)}{\partial M}=0.$

- (1+1)-d NJL model: One can easily carry out the numerical integral on a classical computer **without worrying about the sign problem** with Monte Carlo methods.

- We chose μ, T in the range [0, 300] MeV using the model parameters $m=100$ MeV and $g=1,\ a=1\ \text{MeV}^{-1}$ at $\mu_5=0$.

- $M\to m$ as expected since the NJL model is an asymptotically free model.

- At asymptotically high T or μ, we expect to recover a free field theory.

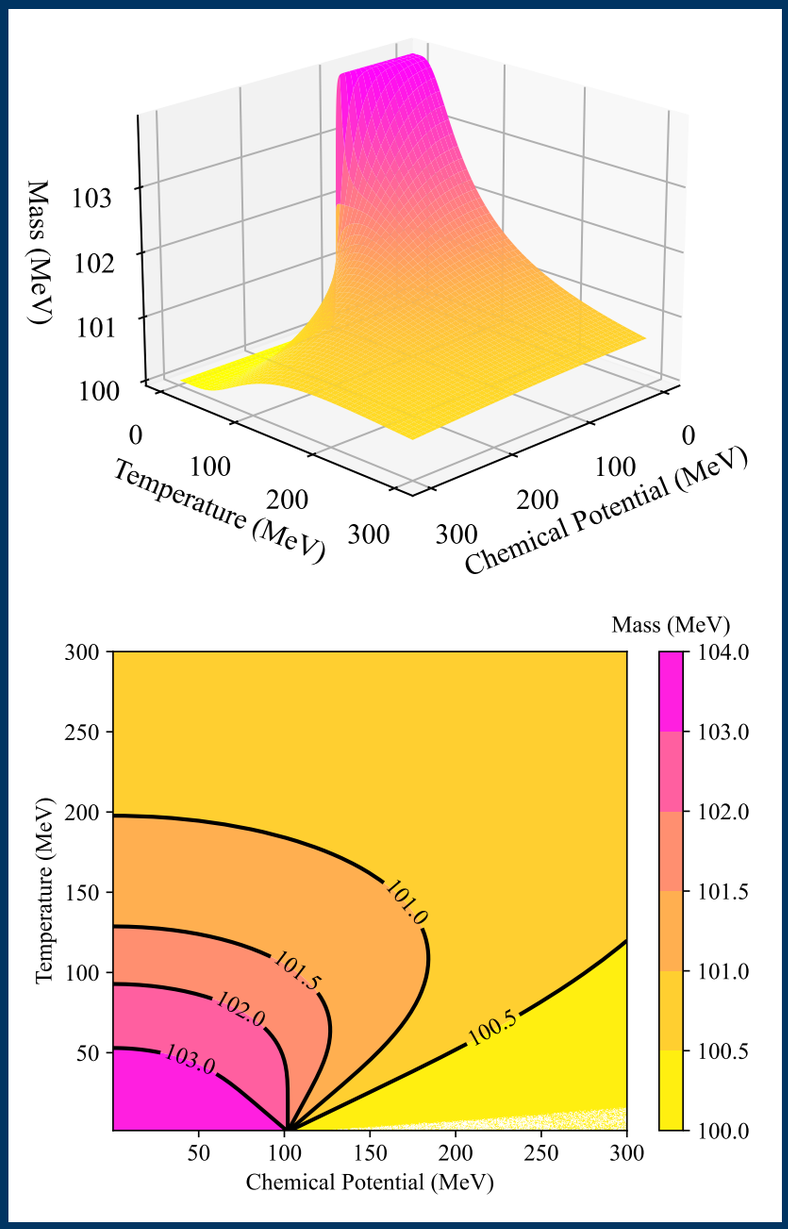

Discretization of the NJL Hamiltonian:

Ingredients of the quantum algorithms

- Starting from the Lagrangian density

$$\mathscr{L} = \bar{\psi}(i\gamma_\mu \partial^\mu - m)\psi + g(\bar{\psi}\psi)^2 + \mu\bar{\psi}\gamma_0\psi + \mu_5\bar{\psi}\gamma_0\gamma_5\psi$$

The NJL Hamiltonian density is

$$\mathscr{H} = \bar{\psi}(i\gamma_1 \partial_1 + m)\psi - g(\bar{\psi}\psi)^2 - \mu\bar{\psi}\gamma_0\psi - \mu_5\bar{\psi}\gamma_0\gamma_5\psi$$

- Given a Dirac fermion field $\psi(x)$ with two components, we show the discretization of the NJL Hamiltonian in the lattice form suitable for a digital quantum simulation by

(1) Writing the Dirac fermion field in terms of the staggered fermion field as applied in lattice QCD: we assign $2n$ sites to the staggered fermion field[J. Kogut and L. Susskind, 1975] :

$$\psi(x = n) = \begin{pmatrix} \chi_{2n} \\ \chi_{2n+1} \end{pmatrix}$$

Discretization of the NJL Hamiltonian:

Ingredients of the quantum algorithms

(1) Given a Dirac fermion field $\psi(x)$ with two components, we assign $2n$ sites to the staggered fermion field[J. Kogut and L. Susskind, 1975] :

$$\psi(x=n)=\begin{pmatrix}\chi_{2n}\\ \chi_{2n+1}\end{pmatrix}$$

(2) Then, for the purpose of quantum simulation, we apply the **Jordan-Wigner transformation**[P. Jordan and E. Wigner, 1928] to convert staggered fermion field to spin representation, namely each staggered fermion field is given by a string a Pauli matrices,

$$\chi_n=\frac{X_n-iY_n}{2}\prod_{i=0}^{n-1}(-iZ_i)$$

where the subscripts indicate the index of qubit where the single-qubit gates are acting on. Therefore, the Hamiltonian in spin representation is given.

Nambu-Jona-Lasinio (NJL) model

- $\mathscr{H} = \bar{\psi}(i\gamma_1\partial_1 + m)\psi - g(\bar{\psi}\psi)^2 - \mu\bar{\psi}\gamma_0\psi - \mu_5\bar{\psi}\gamma_0\gamma_5\psi$

$$\int dx\bar{\psi}i\gamma_1\partial_1\psi = -\frac{i}{2a}\sum_{n=0}^{N-1}\left[\chi_n^\dagger\chi_{n+1} - \chi_{n+1}^\dagger\chi_n\right] = \sum_{n=0}^{N-1}\frac{1}{4a}\left(X_nX_{n+1} + Y_nY_{n+1}\right),$$

$$\int dx\bar{\psi}\psi = \sum_{n=0}^{N-1}(-1)^n\chi_n^\dagger\chi_n = \sum_{n=0}^{N-1}(-1)^n\frac{Z_n}{2},$$

$$\int dx(\bar{\psi}\psi)^2 = \frac{1}{a}\sum_{n=0}^{N/2-1}\left[\chi_{2n}^\dagger\chi_{2n} - \chi_{2n+1}^\dagger\chi_{2n+1}\right]^2 = -\frac{1}{2a}\left[\sum_{n=0}^{N/2-1}(1+Z_{2n})(1+Z_{2n+1}) - \sum_{n=0}^{N-1}(1+Z_n)\right],$$

$$\int dx\bar{\psi}\gamma_0\psi = \sum_{n=0}^{N-1}\chi_n^\dagger\chi_n = \sum_{n=0}^{N-1}\frac{Z_n}{2},$$

$$\int dx\bar{\psi}\gamma_0\gamma_5\psi = -\sum_{n=0}^{N/2-1}(\chi_{2n}^\dagger\chi_{2n+1} + \chi_{2n+1}^\dagger\chi_{2n}) = \frac{1}{2}\sum_{n=0}^{N/2-1}(X_{2n}Y_{2n+1} - Y_{2n}X_{2n+1}),$$

Dirac fermion

So each part of the Hamiltonian can be first written in the form of the Dirac fermion fields as shown in the purple background.

Nambu-Jona-Lasinio (NJL) model

- $\mathscr{H} = \bar{\psi}(i\gamma_1\partial_1 + m)\psi - g(\bar{\psi}\psi)^2 - \mu\bar{\psi}\gamma_0\psi - \mu_5\bar{\psi}\gamma_0\gamma_5\psi$

$$\int dx\bar{\psi}i\gamma_1\partial_1\psi = -\frac{i}{2a}\sum_{n=0}^{N-1}\left[\chi_n^\dagger\chi_{n+1} - \chi_{n+1}^\dagger\chi_n\right] = \sum_{n=0}^{N-1}\frac{1}{4a}\left(X_nX_{n+1} + Y_nY_{n+1}\right),$$

$$\int dx\bar{\psi}\psi = \sum_{n=0}^{N-1}(-1)^n\chi_n^\dagger\chi_n = \sum_{n=0}^{N-1}(-1)^n\frac{Z_n}{2},$$

$$\int dx(\bar{\psi}\psi)^2 = -\frac{1}{a}\sum_{n=0}^{N/2-1}\left[\chi_{2n}^\dagger\chi_{2n} - \chi_{2n+1}^\dagger\chi_{2n+1}\right]^2 = -\frac{1}{2a}\left[\sum_{n=0}^{N/2-1}(1+Z_{2n})(1+Z_{2n+1}) - \sum_{n=0}^{N-1}(1+Z_n)\right],$$

$$\int dx\bar{\psi}\gamma_0\psi = \sum_{n=0}^{N-1}\chi_n^\dagger\chi_n = \sum_{n=0}^{N-1}\frac{Z_n}{2},$$

$$\int dx\bar{\psi}\gamma_0\gamma_5\psi = -\sum_{n=0}^{N/2-1}(\chi_{2n}^\dagger\chi_{2n+1} + \chi_{2n+1}^\dagger\chi_{2n}) = \frac{1}{2}\sum_{n=0}^{N/2-1}(X_{2n}Y_{2n+1} - Y_{2n}X_{2n+1}),$$

staggered fermion

Next transformed to staggered fermion fields on lattice as shown in blue

Nambu-Jona-Lasinio (NJL) model

- $\mathscr{H} = \bar{\psi}(i\gamma_1\partial_1 + m)\psi - g(\bar{\psi}\psi)^2 - \mu\bar{\psi}\gamma_0\psi - \mu_5\bar{\psi}\gamma_0\gamma_5\psi$

$$\int dx\bar{\psi}i\gamma_1\partial_1\psi = -\frac{i}{2a}\sum_{n=0}^{N-1}\left[\chi_n^\dagger\chi_{n+1} - \chi_{n+1}^\dagger\chi_n\right] = \sum_{n=0}^{N-1}\frac{1}{4a}\left(X_nX_{n+1} + Y_nY_{n+1}\right),$$

$$\int dx\bar{\psi}\psi = \sum_{n=0}^{N-1}(-1)^n\chi_n^\dagger\chi_n = \sum_{n=0}^{N-1}(-1)^n\frac{Z_n}{2},$$

$$\int dx(\bar{\psi}\psi)^2 = \frac{1}{a}\sum_{n=0}^{N/2-1}\left[\chi_{2n}^\dagger\chi_{2n} - \chi_{2n+1}^\dagger\chi_{2n+1}\right]^2 = -\frac{1}{2a}\left[\sum_{n=0}^{N/2-1}(1+Z_{2n})(1+Z_{2n+1}) - \sum_{n=0}^{N-1}(1+Z_n)\right],$$

$$\int dx\bar{\psi}\gamma_0\psi = \sum_{n=0}^{N-1}\chi_n^\dagger\chi_n = \sum_{n=0}^{N-1}\frac{Z_n}{2},$$

$$\int dx\bar{\psi}\gamma_0\gamma_5\psi = -\sum_{n=0}^{N/2-1}(\chi_{2n}^\dagger\chi_{2n+1} + \chi_{2n+1}^\dagger\chi_{2n}) = \frac{1}{2}\sum_{n=0}^{N/2-1}(X_{2n}Y_{2n+1} - Y_{2n}X_{2n+1}),$$

spin representation

Then further transformed to spin Hamiltonian, which can be directly represented by quantum gates. Here the subscripts indicate the index of qubit where the single-qubit gates are acting on.

- Eventually, our goal is to compute the QCD phase diagram. Since traditional lattice QCD method has sign issues, we try to explore the application of quantum computing on this problem

- Meanwhile, for this simplified model, numerical calculations can be directly carried out to give exact results for comparison with quantum simulations, without worrying about the sign problem in Monte Carlo methods.

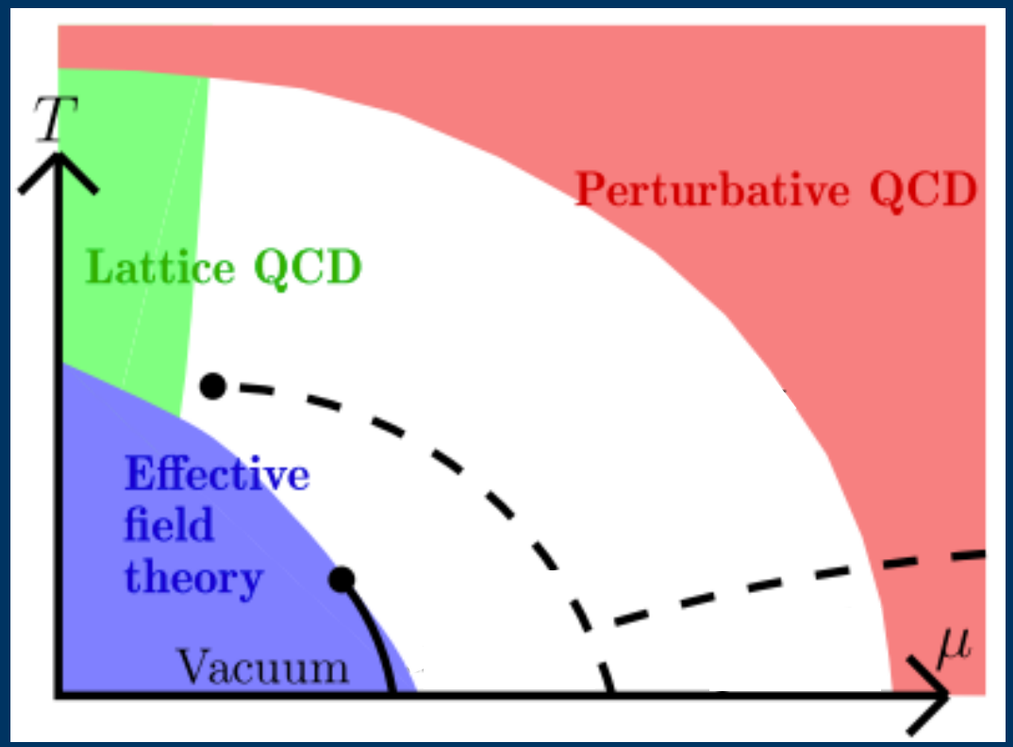

Quantum Simulation of Phase Transitions

- Background
- Nambu-Jona-Lasinio (NJL) model
- Quantum Imaginary Time Evolution (QITE)
- Results
- Summary

Discretization of Hamiltonian

⇓

Quantum simulation

for finite T

Quantum Imaginary Time Evolution (QITE)

- Evolution from $\beta = 0$ state under a Hamiltonian H with a normalization: $|\Psi(\beta)\rangle = \dfrac{e^{-\beta H}}{\sqrt{c(\beta)}} |\Psi(0)\rangle$,

where the normalization $c(\beta) = \langle\Psi(0)| e^{-2\beta H} |\Psi(0)\rangle$, $\beta = 1/T$.

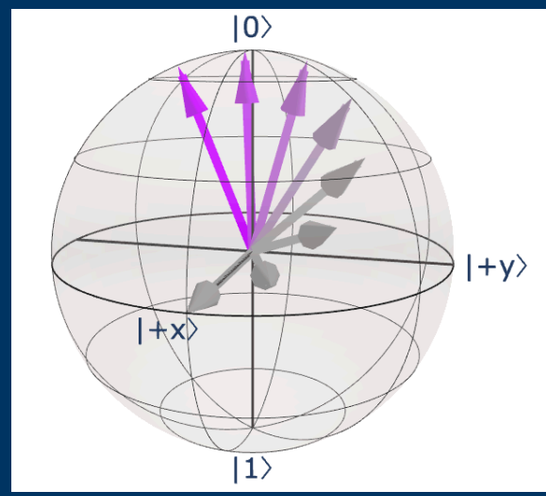

Quantum Imaginary Time Evolution (QITE)

- Evolution from $\beta = 0$ state under a Hamiltonian H with a normalization: $|\Psi(\beta)\rangle = \dfrac{e^{-\beta H}}{\sqrt{c(\beta)}}|\Psi(0)\rangle$,

where the normalization $c(\beta) = \langle\Psi(0)|e^{-2\beta H}|\Psi(0)\rangle$, $\beta = 1/T$.

- In quantum computing, only unitary operator can be implemented:

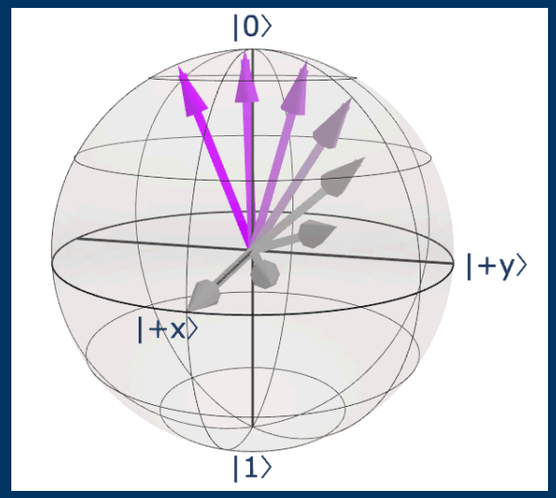

$$\hat{H}|\psi\rangle = i\hbar\frac{\partial}{\partial t}|\psi\rangle$$

Initial

Quantum state

$|\psi(t=0)\rangle$

Final

Quantum state

$|\psi(t)\rangle = e^{-i\hat{H}t/\hbar}|\psi(t=0)\rangle$

unitary operator

Quantum Imaginary Time Evolution (QITE)

- Evolution from $\beta = 0$ state under a Hamiltonian H with a normalization: $|\Psi(\beta)\rangle = \dfrac{e^{-\beta H}}{\sqrt{c(\beta)}}|\Psi(0)\rangle$,

where the normalization $c(\beta) = \langle\Psi(0)|e^{-2\beta H}|\Psi(0)\rangle$, $\beta = 1/T$.

- In quantum computing, only unitary operator can be implemented:

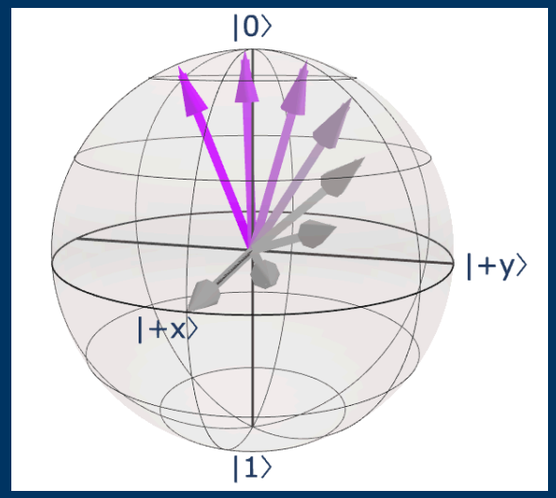

Initial

Quantum state

$|\psi(t=0)\rangle$

$$\hat{H}|\psi\rangle = i\hbar\frac{\partial}{\partial t}|\psi\rangle$$

Final

Quantum state

$|\psi(t)\rangle = e^{-i\hat{H}t/\hbar}|\psi(t=0)\rangle$

Quantum Circuit	**Quantum Mechanics**
Initial qubit array $\leftrightarrow$	$\lvert\psi(t=0)\rangle$
Quantum gate array $\leftrightarrow$	$e^{-i\hat{H}t/\hbar}$

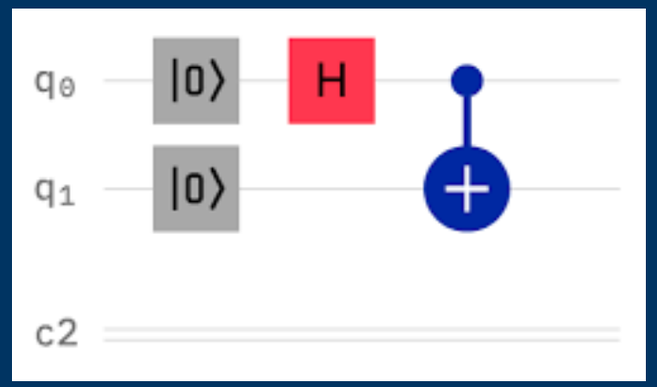

Quantum Imaginary Time Evolution (QITE)

- Evolution from $\beta = 0$ state under a Hamiltonian H with a normalization: $|\Psi(\beta)\rangle = \dfrac{e^{-\beta H}}{\sqrt{c(\beta)}} |\Psi(0)\rangle$,

where the normalization $c(\beta) = \langle\Psi(0)| e^{-2\beta H} |\Psi(0)\rangle$, $\beta = 1/T$.

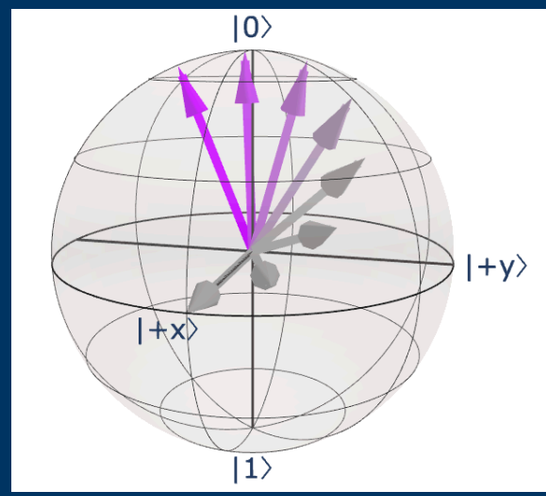

★ The operator $e^{-\beta H}$ is **non-unitary** ⇒ cannot be implemented on a quantum circuit

⇒ Need a method to convert this non-unitary operator into a unitary operator that could be applied to a quantum circuit

Quantum Imaginary Time Evolution (QITE)

- Evolution from $\beta = 0$ state under a Hamiltonian H with a normalization: $|\Psi(\beta)\rangle = \dfrac{e^{-\beta H}}{\sqrt{c(\beta)}} |\Psi(0)\rangle$,

where the normalization $c(\beta) = \langle\Psi(0)| e^{-2\beta H} |\Psi(0)\rangle$, $\beta = 1/T$.

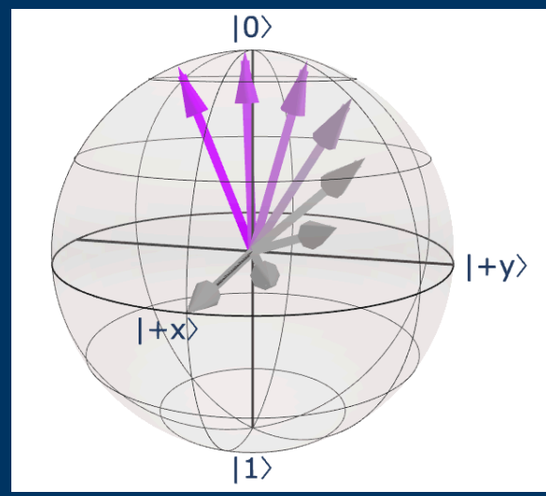

★ The operator $e^{-\beta H}$ is **non-unitary** ⇒ cannot be implemented on a quantum circuit

⇒ Need a method to convert this non-unitary operator into a unitary operator that could be applied to a quantum circuit

Quantum imaginary time evolution (QITE) algorithm [Mario Motta, et al, *Nature Physics, 2020*]

⇒ Calculate the thermal properties of the NJL Hamiltonian at finite T

- We first decompose the imaginary time evolution operator $e^{-\beta H}$ into $N = \beta/\Delta\beta$ steps:

$$e^{-\beta H} = \left(e^{-\Delta\beta H}\right)^N + O(\Delta\beta^2)$$

Then the thermal state at $\beta + \Delta\beta$ is evolved from the state at β with a small step:

$$|\Psi(\beta + \Delta\beta)\rangle = \frac{e^{-\Delta\beta H}}{\sqrt{c(\Delta\beta)}} |\Psi(\beta)\rangle \, .$$

State preparation (separated into N steps):

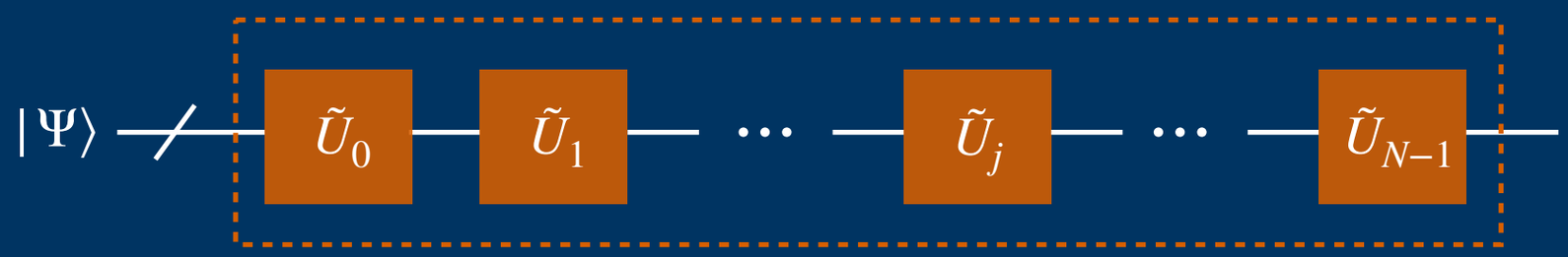

Non-unitary:

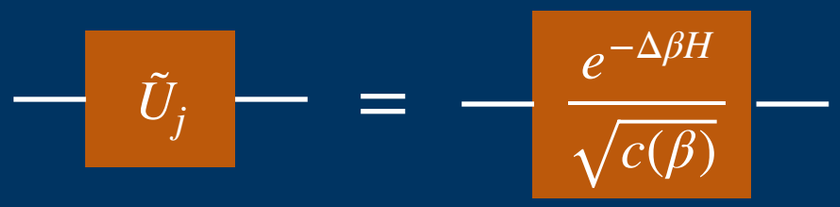

Quantum Imaginary Time Evolution (QITE)

State preparation (separated into N steps):

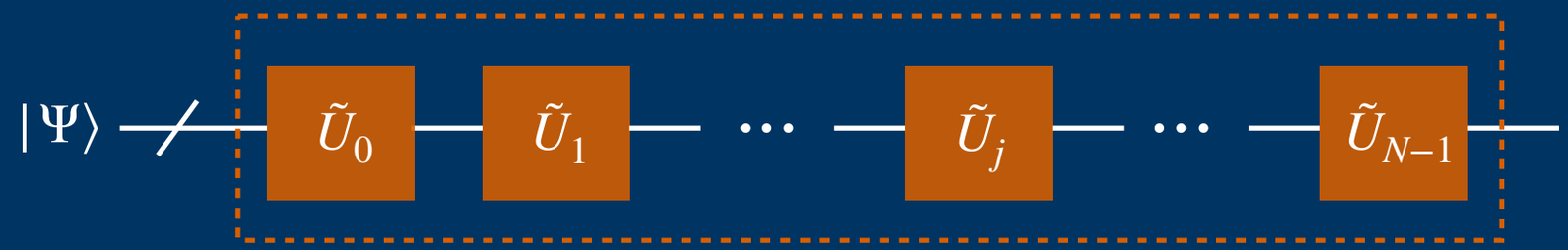

Non-unitary:

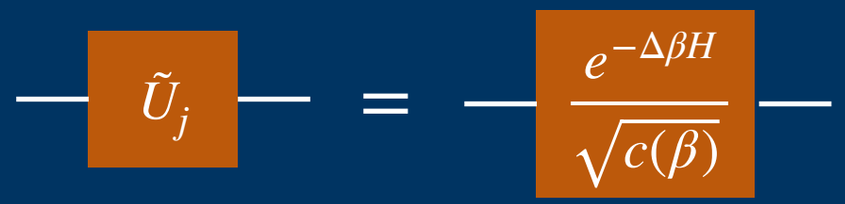

To perform the above operation on a quantum circuit, we approximate the non-unitary evolution $e^{-\Delta\beta H}$ with a unitary operation $e^{-i\Delta\beta A}$, s.t.

$$\frac{1}{\sqrt{c(\Delta\beta)}} e^{-\Delta\beta H} |\Psi(\beta)\rangle \approx e^{-i\Delta\beta A} |\Psi(\beta)\rangle,$$

where $c(\Delta\beta) = \langle\Psi(\beta)| e^{-2\Delta\beta H} |\Psi(\beta)\rangle$

⇒ Same effects when acting on a quantum state for $\Delta\beta$

- We parametrized the Hermitian operator A with a linear combination of Pauli operators with a_μ: a composite parameter

  (runs over all possible combinations of the Pauli gates acting on all the qubits)

$$A(\boldsymbol{a}) = \sum_{\mu}^{N_\mu} a_\mu \sigma_\mu = \sum_{i_0,\cdots,i_{n_q-1}} a_{i_0,\cdots,i_{n_q-1}} \sigma_{i_0} \cdots \sigma_{i_{n_q-1}}$$

- Next we need to minimize the objective function given by an inner product

$F(a) = \left|\left| |\Delta\Psi_H(\beta)\rangle - |\Delta\Psi_A(\beta)\rangle \right|\right|^2$, where

$$|\Delta\Psi(\beta)\rangle = \frac{1}{\Delta\beta}\left(|\Psi(\beta+\Delta\beta)\rangle - |\Psi(\beta)\rangle\right)$$

- We parametrized the Hermitian operator A with a linear combination of Pauli operators with a_μ: a composite parameter

  (runs over all possible combinations of the Pauli gates acting on all the qubits)

$$A(\boldsymbol{a}) = \sum_{\mu}^{N_\mu} a_\mu \sigma_\mu = \sum_{i_0,\cdots,i_{n_q-1}} a_{i_0,\cdots,i_{n_q-1}} \sigma_{i_0} \cdots \sigma_{i_{n_q-1}}$$

- Next we need to minimize the objective function given by an inner product

$$F(a) = \left|\left| \, |\Delta\Psi_H(\beta)\rangle - |\Delta\Psi_A(\beta)\rangle \right|\right|^2, \text{ where}$$

$$|\Delta\Psi(\beta)\rangle = \frac{1}{\Delta\beta}\left(|\Psi(\beta+\Delta\beta)\rangle - |\Psi(\beta)\rangle\right)$$

$$|\Delta\Psi_H(\beta)\rangle = \frac{1}{\Delta\beta}\left(\frac{1}{\sqrt{c(\Delta\beta)}} e^{-\Delta\beta H}|\Psi(\beta)\rangle - |\Psi(\beta)\rangle\right)$$

$|\Psi(\beta+\Delta\beta)\rangle$

change rate of quantum state evolved by $e^{-\beta H}$

- We parametrized the Hermitian operator A with a linear combination of Pauli operators with a_μ: a composite parameter

  (runs over all possible combinations of the Pauli gates acting on all the qubits)

$$A(\boldsymbol{a}) = \sum_{\mu}^{N_\mu} a_\mu \sigma_\mu = \sum_{i_0,\cdots,i_{n_q-1}} a_{i_0,\cdots,i_{n_q-1}} \sigma_{i_0} \cdots \sigma_{i_{n_q-1}}$$

- Next we need to minimize the objective function given by an inner product

$$F(a) = \left| \, |\Delta\Psi_H(\beta)\rangle - |\Delta\Psi_A(\beta)\rangle \, \right|^2, \text{ where}$$

$$|\Delta\Psi(\beta)\rangle = \frac{1}{\Delta\beta}\Big(|\Psi(\beta+\Delta\beta)\rangle - |\Psi(\beta)\rangle \Big)$$

$$|\Delta\Psi_H(\beta)\rangle = \frac{1}{\Delta\beta}\left(\frac{1}{\sqrt{c(\Delta\beta)}} e^{-\Delta\beta H} |\Psi(\beta)\rangle - |\Psi(\beta)\rangle \right)$$

$$|\Psi(\beta+\Delta\beta)\rangle$$

change rate of quantum state evolved by $e^{-\beta H}$

$$|\Delta\Psi_A(\beta)\rangle = \frac{1}{\Delta\beta}\left(e^{-i\Delta\beta A} |\Psi(\beta)\rangle - |\Psi(\beta)\rangle \right)$$

$$|\Psi(\beta+\Delta\beta)\rangle$$

change rate of quantum state evolved by $e^{-i\beta A}$

- Next we need to minimize the objective function $F(a)$ given by an inner product $\left|\left| \, |\Delta\Psi_H(\beta)\rangle - |\Delta\Psi_A(\beta)\rangle \, \right|\right|^2$, where

$$|\Delta\Psi_H(\beta)\rangle = \frac{1}{\Delta\beta}\left(\frac{1}{\sqrt{c(\Delta\beta)}} e^{-\Delta\beta H}|\Psi(\beta)\rangle - |\Psi(\beta)\rangle\right) \qquad |\Delta\Psi_A(\beta)\rangle = \frac{1}{\Delta\beta}\left(e^{-i\Delta\beta A}|\Psi(\beta)\rangle - |\Psi(\beta)\rangle\right)$$

★ Then the objective function $F(a)$ is

$$F(a) = \left(\langle\Delta\Psi_H(\beta)| - \langle\Delta_A\Psi(\beta)|\right)\left(|\Delta\Psi_H(\beta)\rangle - |\Delta_A\Psi(\beta)\rangle\right)$$

$$= \langle\Delta\Psi_H(\beta)|\Delta\Psi_H(\beta)\rangle - \sum_\mu b_\mu a_\mu + \sum_{\mu,\nu} a_\mu S_{\mu\nu} a_\nu$$

a-independent function — Linear system of a

$$S_{\mu\nu} = \langle\Psi(\beta)|\sigma_\nu^\dagger\sigma_\mu|\Psi(\beta)\rangle, \qquad b_\mu = -\frac{i}{\sqrt{c(\Delta\beta)}}\langle\Psi(\beta)|\left(\sigma_\mu^\dagger H - H\sigma_\mu\right)|\Psi(\beta)\rangle$$

Constructed from known quantities

- Then the objective function $F(a)$ is

$$F(a) = \left(\langle \Delta\Psi_H(\beta)| - \langle \Delta_A\Psi(\beta)| \right)\left(|\Delta\Psi_H(\beta)\rangle - |\Delta_A\Psi(\beta)\rangle\right)$$

$$= \langle \Delta\Psi_H(\beta)|\Delta\Psi_H(\beta)\rangle - \boxed{\sum_\mu b_\mu a_\mu + \sum_{\mu,\nu} a_\mu S_{\mu\nu} a_\nu}$$

Linear system of a

a-independent function

$$S_{\mu\nu} = \langle\Psi(\beta)|\sigma_\nu^\dagger\sigma_\mu|\Psi(\beta)\rangle,\ b_\mu = -\frac{i}{\sqrt{c(\Delta\beta)}}\langle\Psi(\beta)|\left(\sigma_\mu^\dagger H - H\sigma_\mu\right)|\Psi(\beta)\rangle$$

★ Thus minimizing $F(a)$ with respective to a $\Leftrightarrow$ $\dfrac{dF(a)}{da_\mu} = 0$

$$\Rightarrow\ (\boldsymbol{S} + \boldsymbol{S}^T)\boldsymbol{a} = \boldsymbol{b}$$

- Insert a back to the definition of A:

$$A(\boldsymbol{a}) = \sum_\mu^{N_\mu} a_\mu\sigma_\mu = \sum_{i_0,\cdots,i_{nq-1}} a_{i_0,\cdots,i_{nq-1}}\sigma_{i_0}\cdots\sigma_{i_{nq-1}}$$

- Then the objective function $F(a)$ is

$$F(a) = \left(\langle \Delta\Psi_H(\beta)| - \langle \Delta_A\Psi(\beta)| \right)\left(|\Delta\Psi_H(\beta)\rangle - |\Delta_A\Psi(\beta)\rangle\right)$$

$$= \langle \Delta\Psi_H(\beta)|\Delta\Psi_H(\beta)\rangle - \boxed{\sum_\mu b_\mu a_\mu + \sum_{\mu,\nu} a_\mu S_{\mu\nu} a_\nu}$$

Linear system of a

a-independent function

$$S_{\mu\nu} = \langle\Psi(\beta)|\sigma_\nu^\dagger\sigma_\mu|\Psi(\beta)\rangle,\ b_\mu = -\frac{i}{\sqrt{c(\Delta\beta)}}\langle\Psi(\beta)|\left(\sigma_\mu^\dagger H - H\sigma_\mu\right)|\Psi(\beta)\rangle$$

★ Thus minimizing $F(a)$ with respective to a $\Leftrightarrow$ $\dfrac{dF(a)}{da_\mu} = 0$

$$\Rightarrow\ (\boldsymbol{S} + \boldsymbol{S}^T)\boldsymbol{a} = \boldsymbol{b}$$

- Insert a back to the definition of A:

$$A(\boldsymbol{a}) = \sum_\mu^{N_\mu} a_\mu\sigma_\mu = \sum_{i_0,\cdots,i_{nq-1}} a_{i_0,\cdots,i_{nq-1}}\sigma_{i_0}\cdots\sigma_{i_{nq-1}}$$

$$\frac{1}{\sqrt{c(\Delta\beta)}}e^{-\Delta\beta H}|\Psi(\beta)\rangle \approx e^{-i\Delta\beta A}|\Psi(\beta)\rangle$$

- Now with the non-unitary operator $e^{-\Delta\beta H}$ written in terms of a unitary operator $e^{-i\Delta\beta A}$, we are able to evolve the state to imaginary time β using

$$|\Psi(\beta)\rangle = \frac{\left(e^{-\Delta\beta H}\right)^N}{\sqrt{c(\beta)}}|\Psi(0)\rangle = \left(e^{-i\Delta\beta A}\right)^N|\Psi(0)$$

State preparation:

Unitary:

⇒ All the operators can be implemented on a quantum computer

- To calculate the thermal average of a given observable, we measure the observable between two thermal states.

$$\langle\hat{O}\rangle = \frac{\mathrm{Tr}(e^{-\beta\hat{H}}\hat{O})}{\mathrm{Tr}(e^{-\beta\hat{H}})} = \frac{\langle\Psi(\beta/2)|\hat{O}|\Psi(\beta/2)\rangle}{\langle\Psi(\beta/2)\rangle|\Psi(\beta/2)\rangle}$$

$$|\Psi(\beta)\rangle = \frac{\left(e^{-\Delta\beta H}\right)^N}{\sqrt{c(\beta)}}|\Psi(0)\rangle \approx \left(e^{-i\Delta\beta A}\right)^N|\Psi(0)\rangle$$

- Chiral condensate $\langle\bar{\psi}\psi\rangle$ as a function of β.
- Compare the exact diagonalization (using the discretization of the NJL Hamiltonian) and QITE simulations.

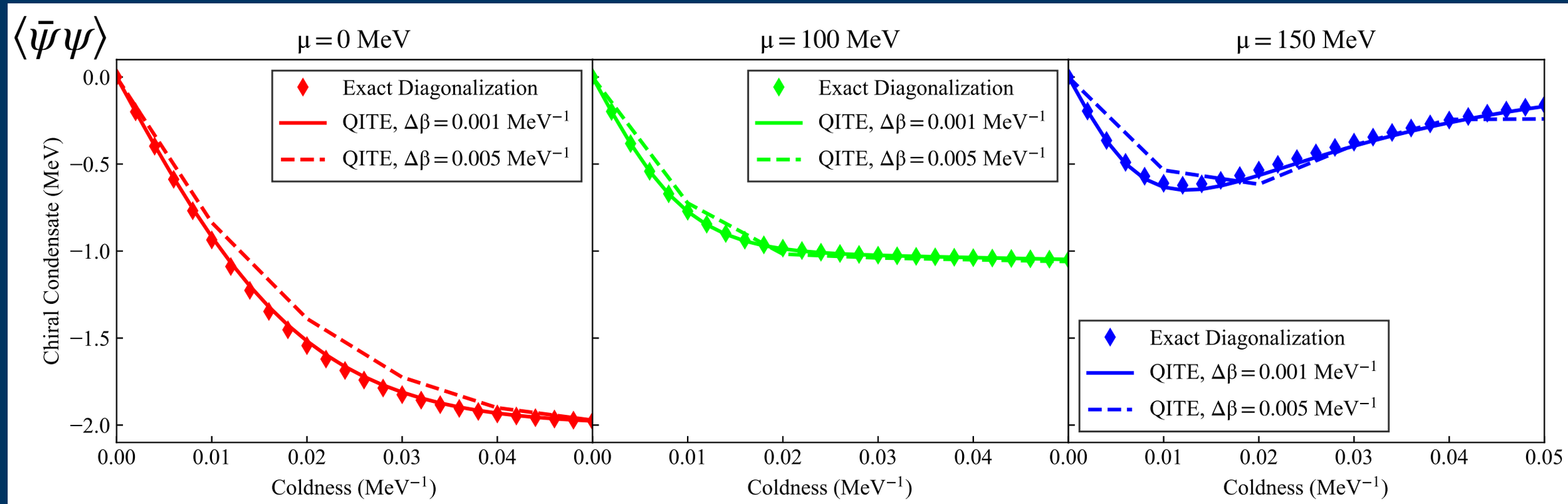

Coupling constant $g = 1$ and the quark mass $m = 100$ MeV on a lattice grid withspacing $a = 1$ MeV^{-1}

$$|\Psi(\beta)\rangle = \frac{\left(e^{-\Delta\beta H}\right)^N}{\sqrt{c(\beta)}}|\Psi(0)\rangle \approx \left(e^{-i\Delta\beta A}\right)^N|\Psi(0)\rangle$$

- Expected by trotterization: more accurate quantum simulations with smaller $\Delta\beta$.
- In the rest of this talk, we will apply step $\Delta\beta = 0.001$/MeV and show the effective mass M at various finite chemical potentials and temperatures.

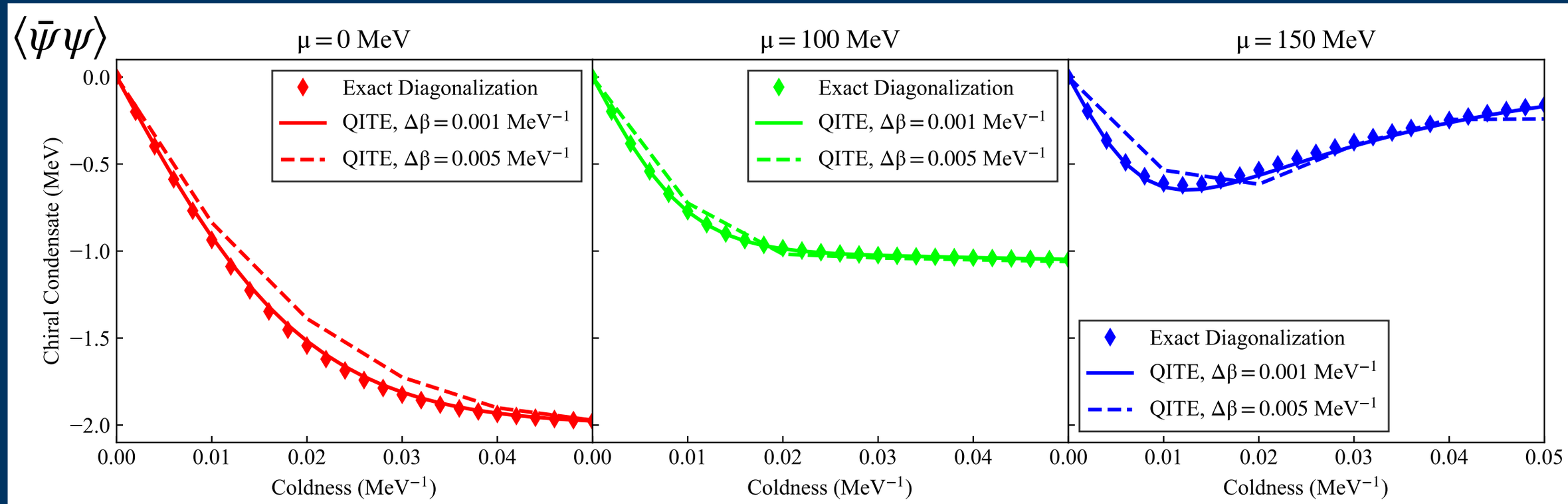

Coupling constant $g = 1$ and the quark mass $m = 100$ MeV on a lattice grid withspacing $a = 1$ MeV^{-1}

Results

★ **Analytical**: By working on a (1+1)-d model, we are able to derive an analytical result by solving the gap equation

$$\frac{\partial \Omega}{\partial M} = 0$$

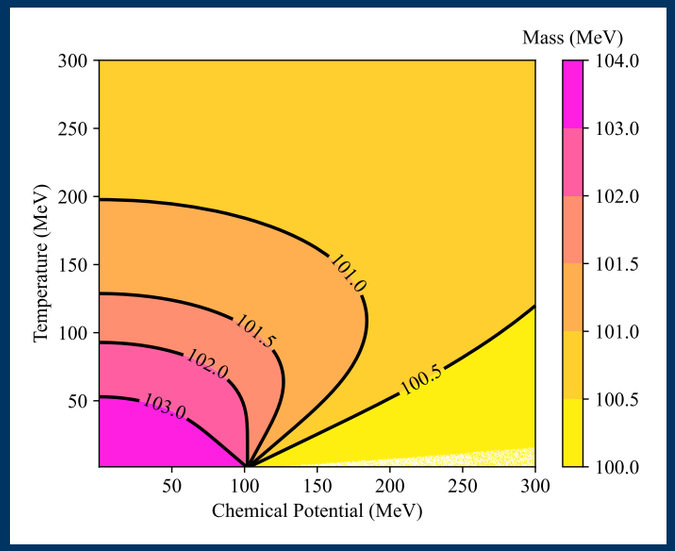

⇒ for comparison to the quantum simulations.

★ **QC**: Restriction on (1+1) d enables us to design a quantum circuit with a small amount of qubits

⇒ feasibility of implementing such circuit on currently available hardwares for further research.

$$|\Psi(\beta)\rangle \approx \left(e^{-i\Delta\beta A}\right)^N |\Psi(0)\rangle$$

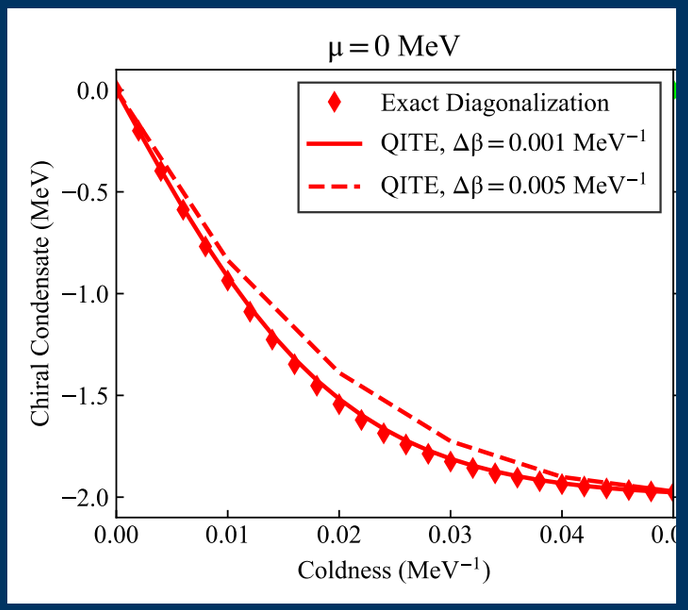

Results

- Demonstrate (1+1)-dimensional NJL chiral phase transition by plotting $\langle\bar{\psi}\psi\rangle$ as a function of T, μ and μ_5 with:

  1. Quantum simulation of the thermal states (**QITE**);
  2. Calculate the observables using Hamiltonian in spin representation (**Exact diagonalization**);
  3. Numerically solving the gap equation $\frac{\partial\Omega}{\partial M}=0$ (**Analytical calculation**).

Parameters that will be used in our work are set as:

lattice spacing $a=1$ MeV^{-1}, bare mass $m=100$ MeV and coupling constant $g=1$.

$\mu_5 = 0$

$$\langle \bar{\psi}\psi \rangle = \frac{m - M}{2g}$$

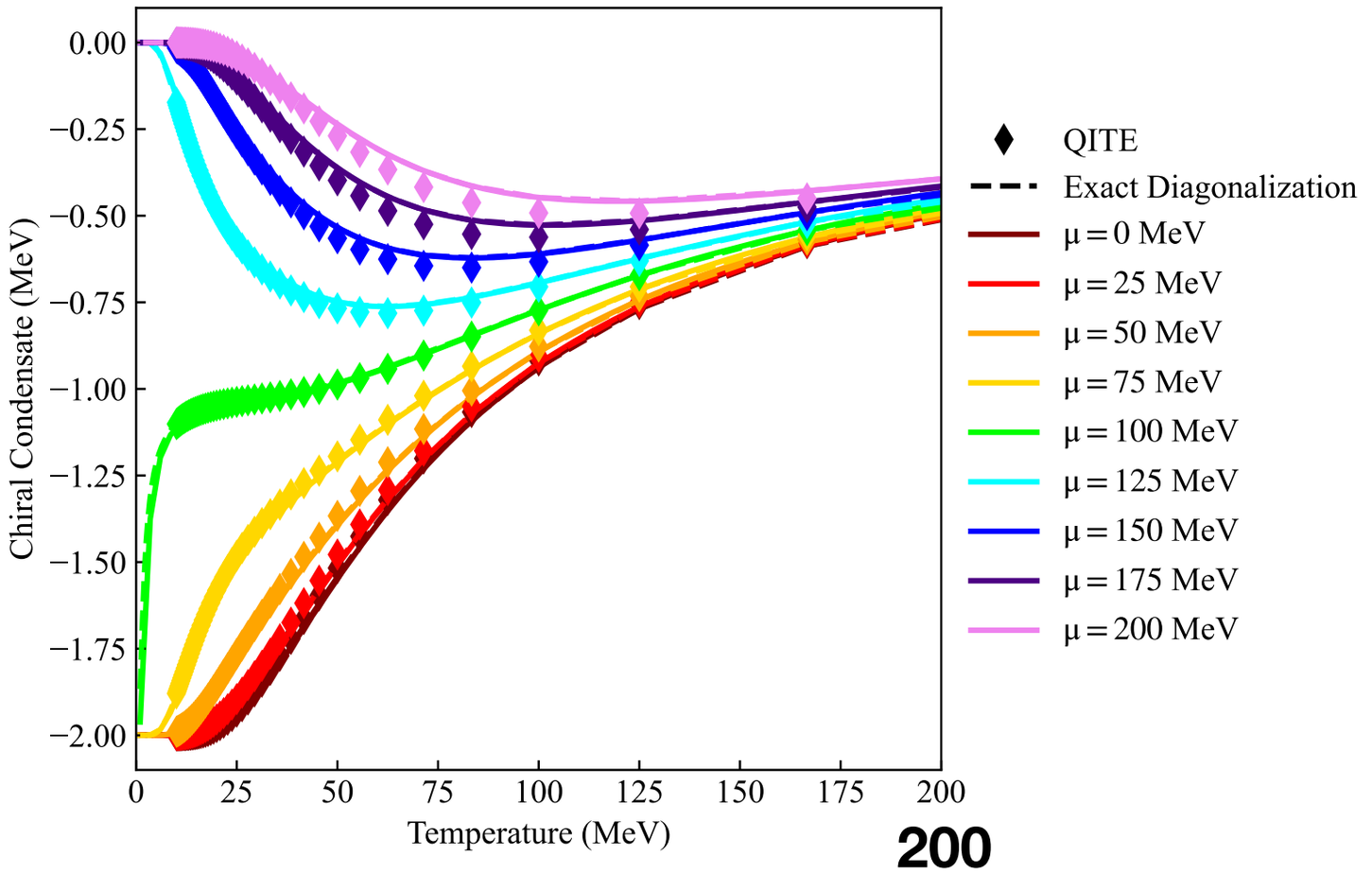

- Consistent results among the three methods

$\mu_5 = 0$

$$\langle \bar{\psi}\psi \rangle = \frac{m - M}{2g}$$

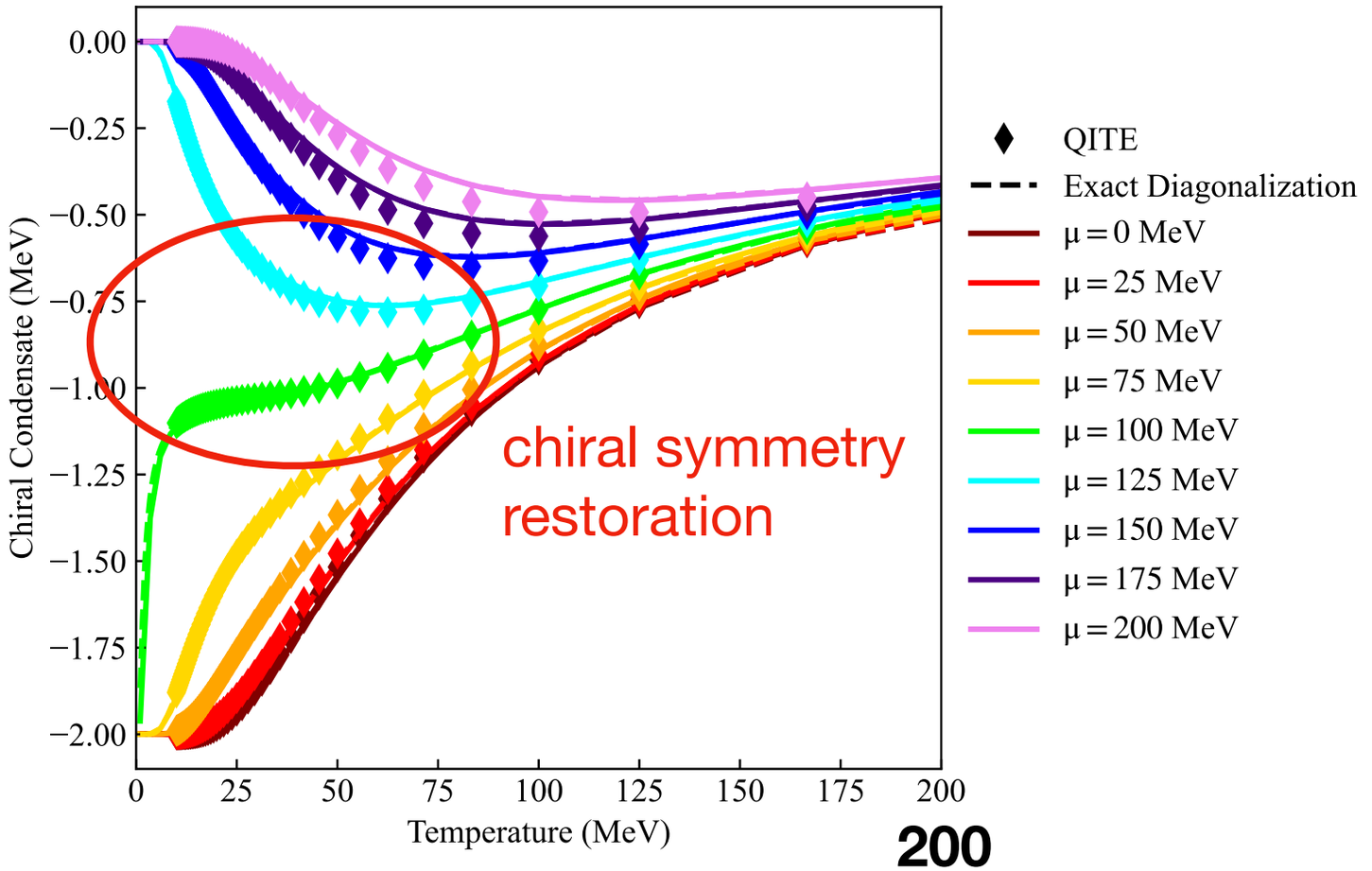

200

- Consistent results among the three methods
- Nontrivial chiral symmetry restoration at $0 < T < 25$ MeV, $100 < \mu < 125$ MeV
- Converge to 0 at larger T as expected by the asymptotic freedom of the NJL model

$\mu_5 = 0$

$$\langle \bar{\psi}\psi \rangle = \frac{m - M}{2g}$$

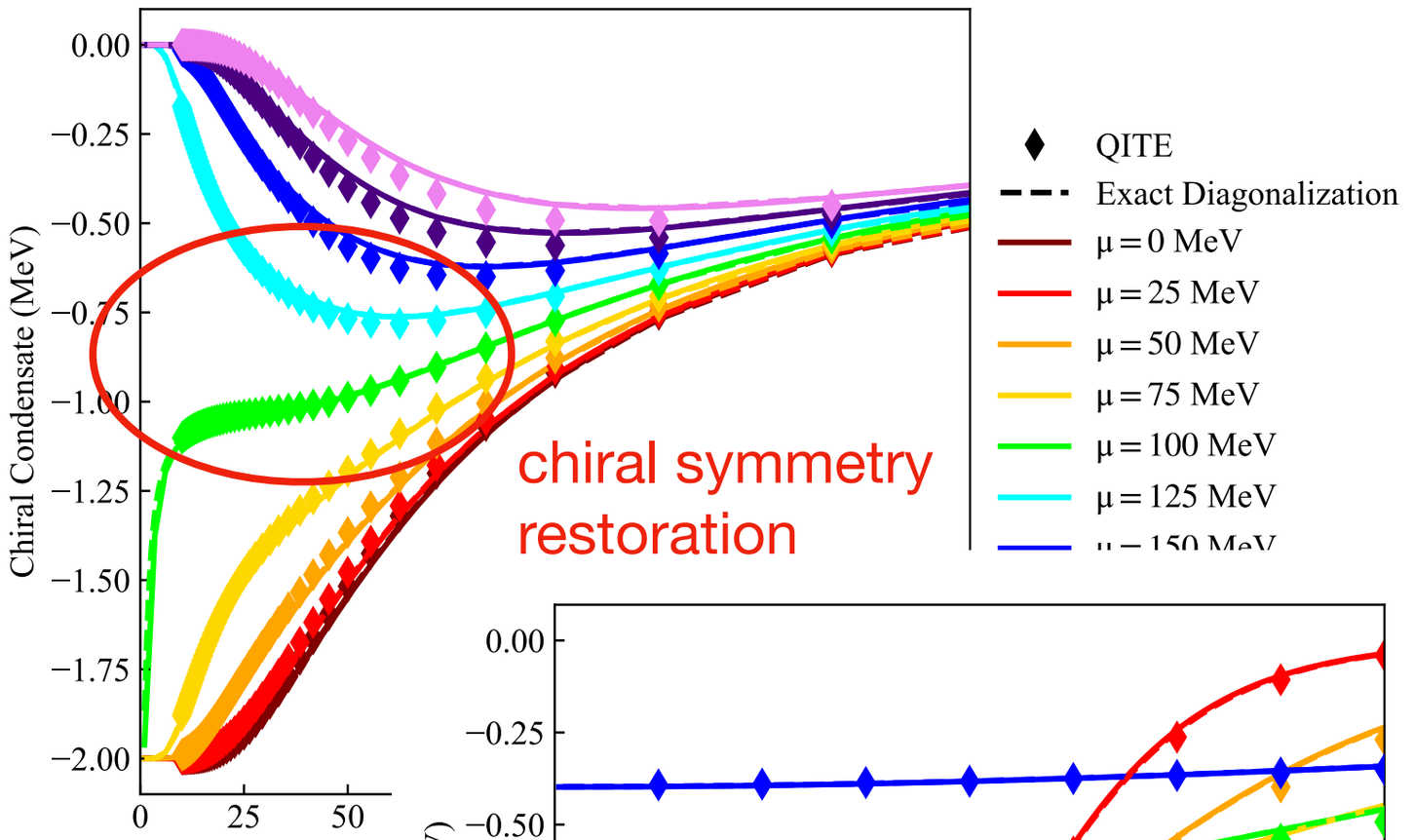

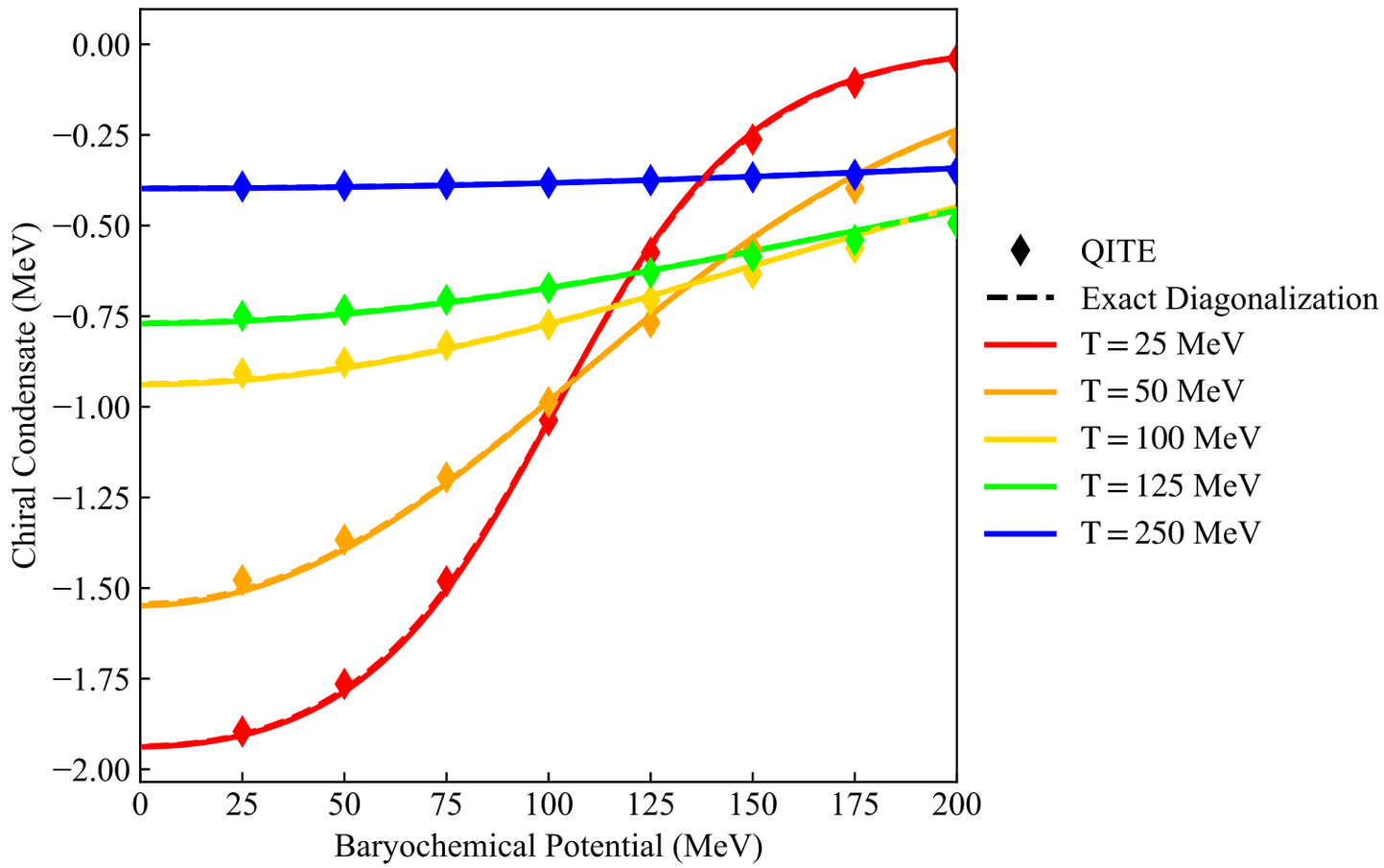

- Consistent results among
- Nontrivial chiral symmetry
- Converge to 0 at larger T a
model

$\mu_5 = 0$

$$\langle \bar{\psi}\psi \rangle = \frac{m - M}{2g}$$

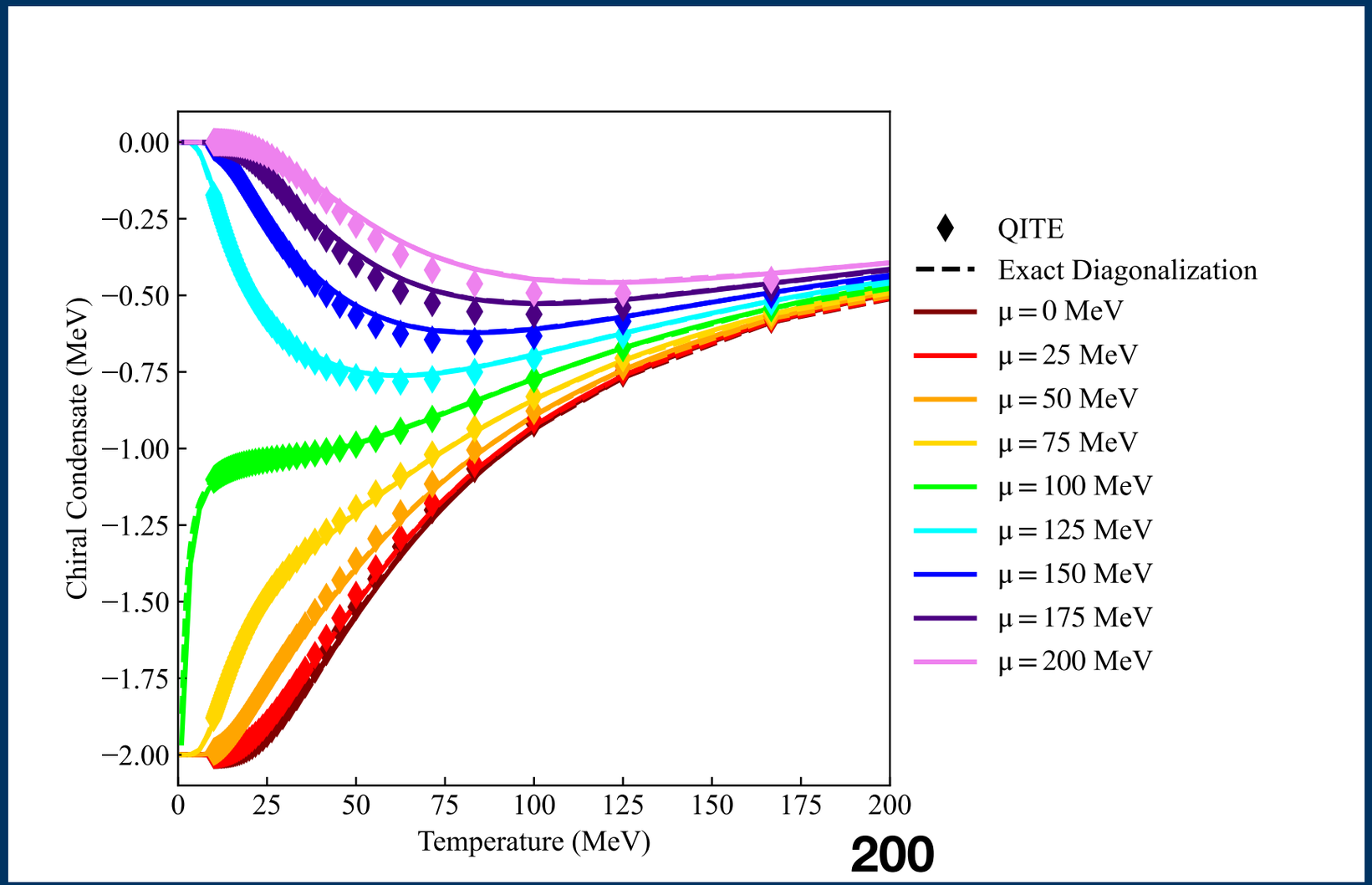

- Consistent results among the three methods
- Nontrivial chiral symmetry restoration at $0 < T < 25$ MeV, $100 < \mu < 125$ MeV
- Converge to 0 at larger T as expected by the asymptotic freedom of the NJL model

$\mu_5 = 0$

$$\langle \bar{\psi}\psi \rangle = \frac{m - M}{2g}$$

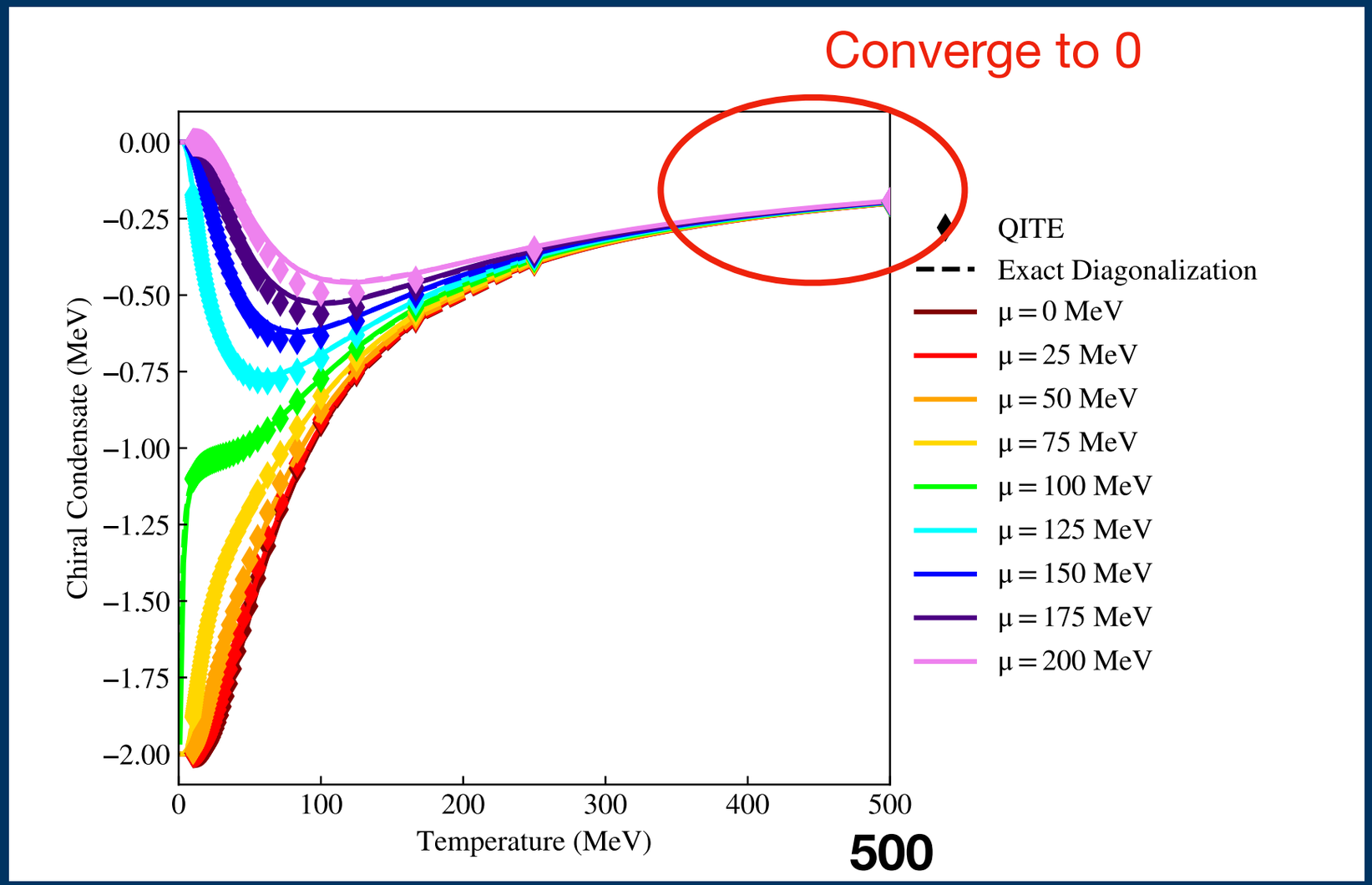

As temperature or chemical potentials increases, the effective mass M tends to be bare mass as expected since the GN model is an asymptotically free model.

$\mu_5 = 0$

$$\langle \bar{\psi}\psi \rangle = \frac{m - M}{2g}$$

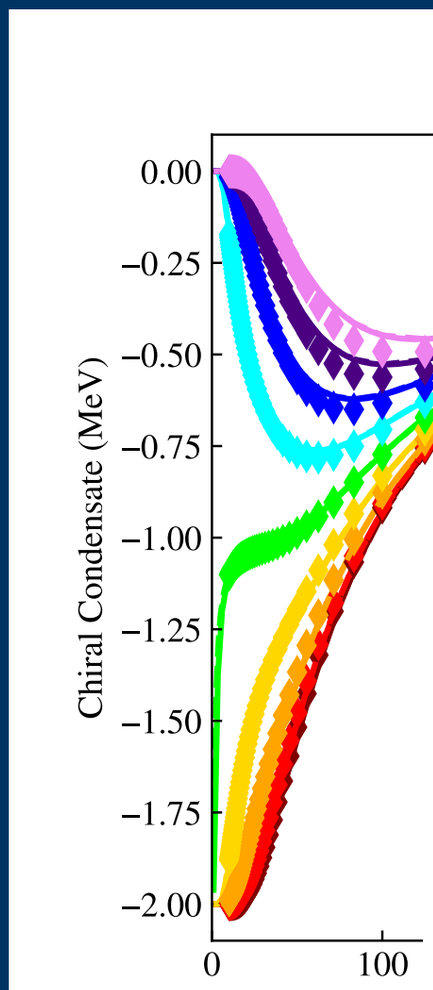

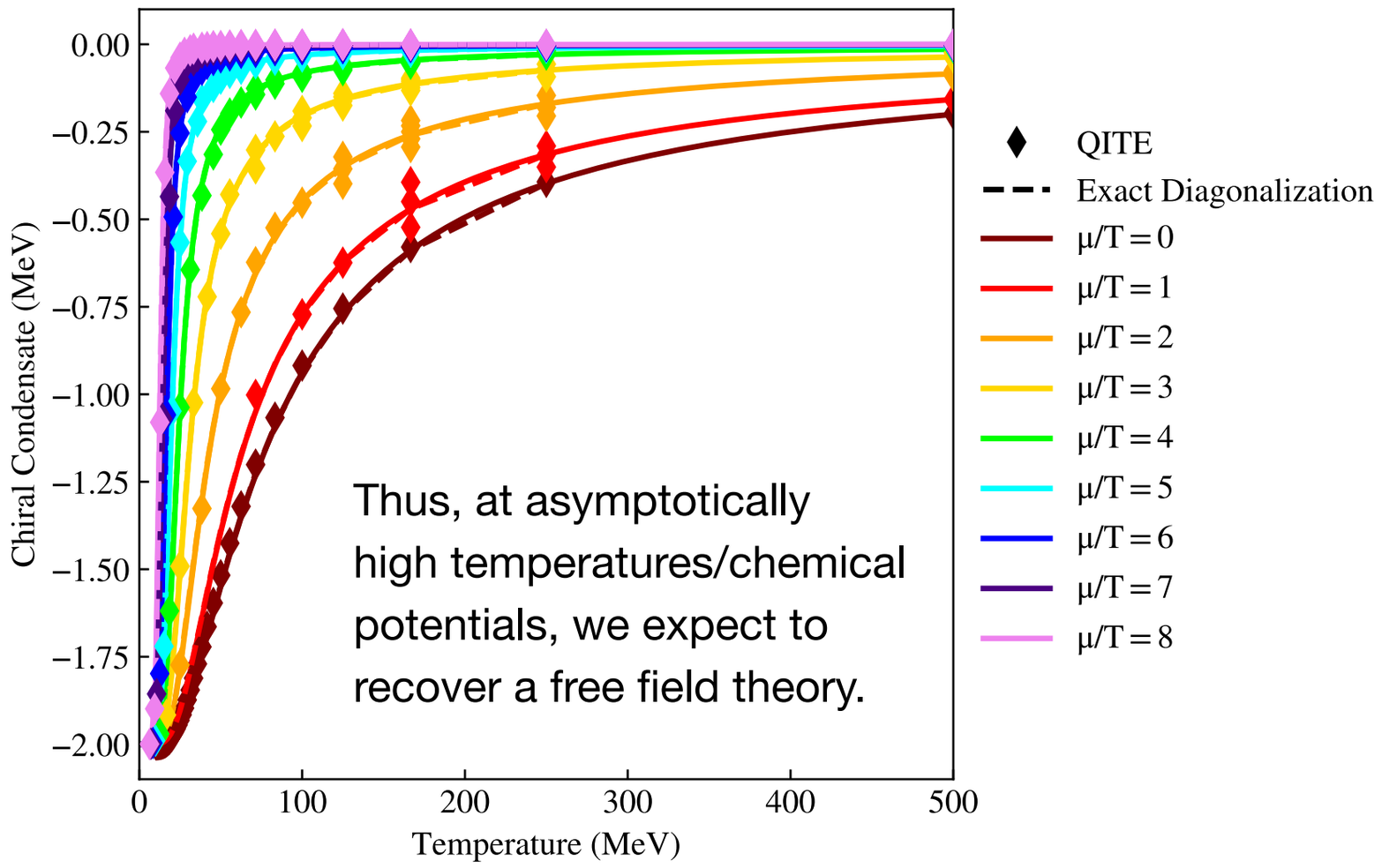

- Consistent results amon
- Nontrivial chiral symmet
- Converge to 0 at larger T
  model

At various values of chiral chemical potentials μ_5 shown in each panel, we plot the effective mass as a function of temperature T at various baryochemical potentials μ at $g = 1$:

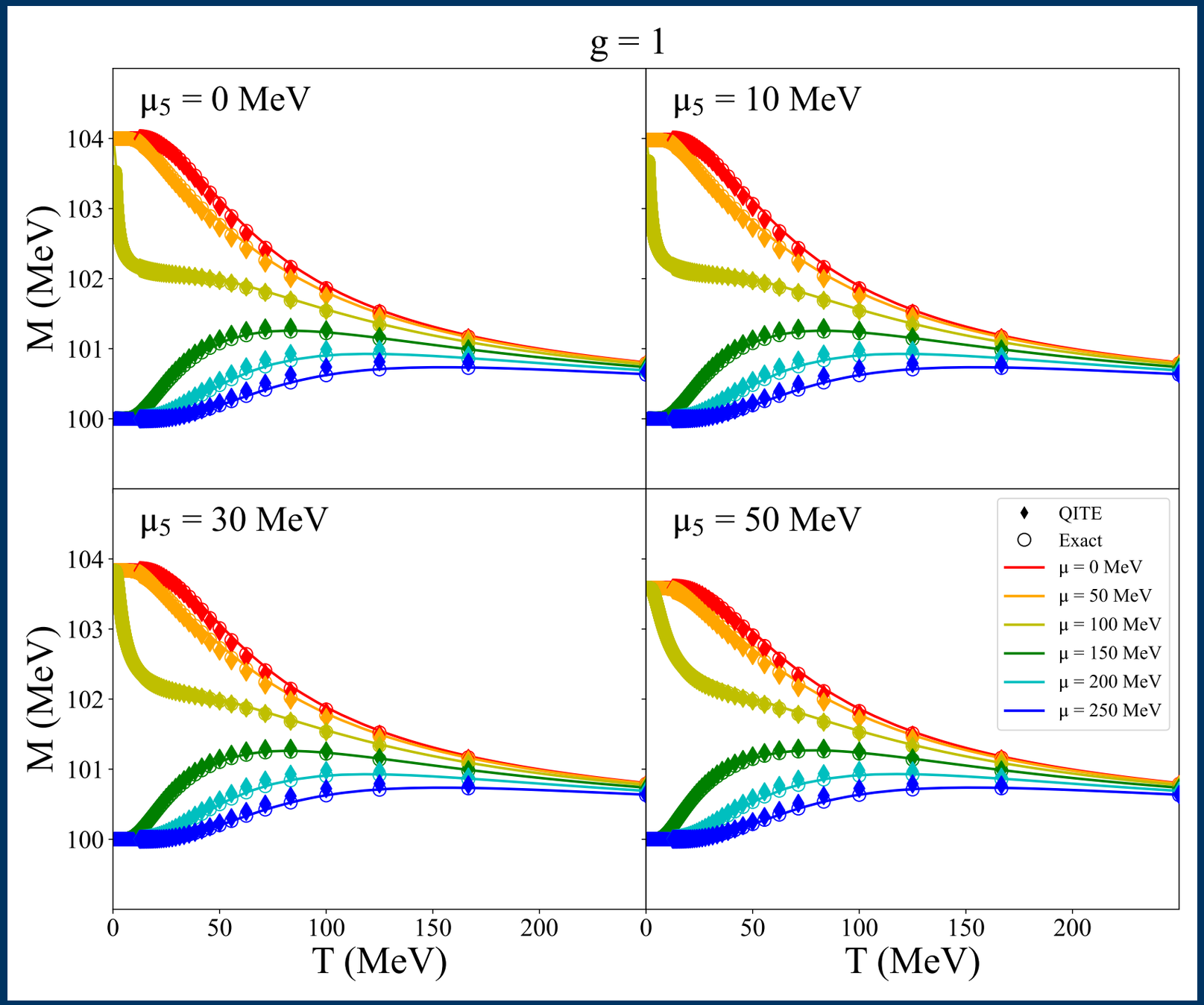

M

- Nontrivial chiral symmetry restoration at $0 < T < 25$ MeV, $100 < \mu < 125$ MeV
- At smaller μ_5, the effective mass M changes more rapidly as a function of T.

Summary

- We have constructed a quantum simulation for the chiral phase transition of the 1+1 dimensional NJL model at finite temperature and chemical potentials with the QITE algorithm

Summary

- We have constructed a quantum simulation for the chiral phase transition of the 1+1 dimensional NJL model at finite temperature and chemical potentials with the QITE algorithm

- We observe a consistency among digital quantum simulation, exact diagonalization and analytical solution, indicating rich applications of quantum computing in simulating finite-temperature behaviors for QCD in the future.

Summary

- We have constructed a quantum simulation for the chiral phase transition of the 1+1 dimensional NJL model at finite temperature and chemical potentials with the QITE algorithm

- We observe a consistency among digital quantum simulation, exact diagonalization and analytical solution, indicating rich applications of quantum computing in simulating finite-temperature behaviors for QCD in the future.

- We expect to use NISQ (Noisy Intermediate-Scale Quantum) computers for producing consistent and correct answers to physical problems, some of which cannot be efficiently solved with classical computing algorithms.

Outlook

- More application of QC in QCD remains to be explored…

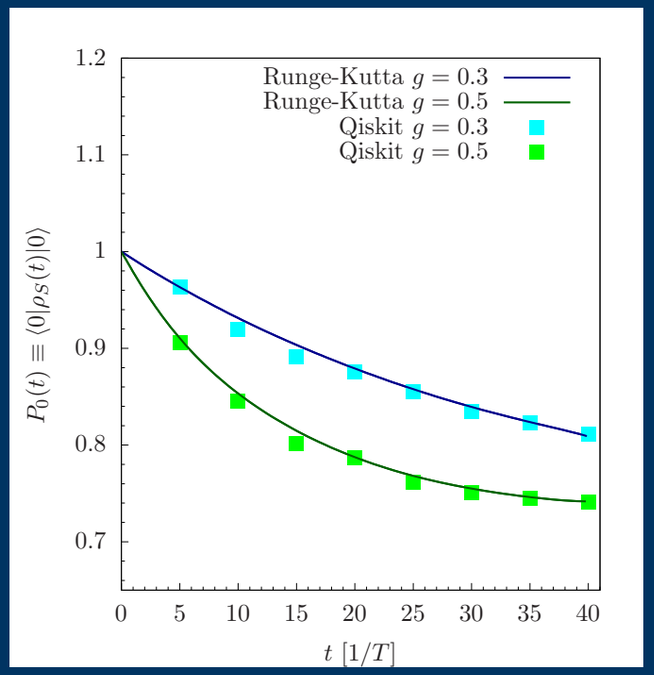

Open quantum system

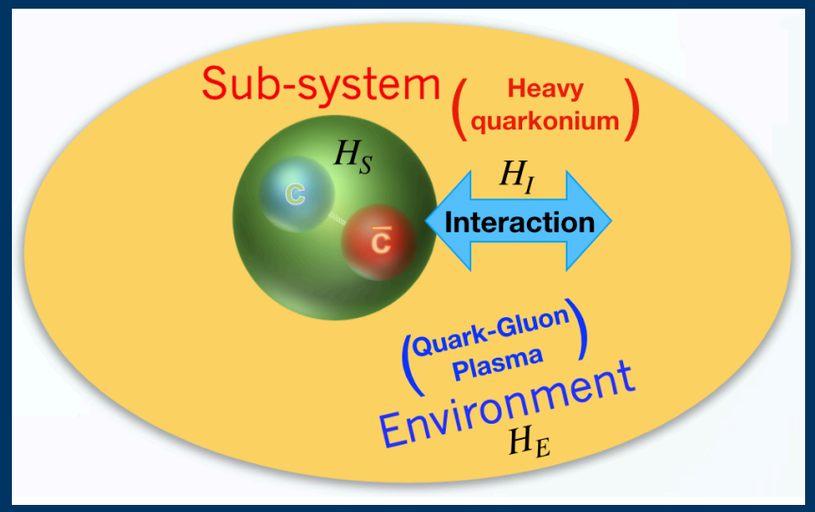

[Wibe A. de Jong et al., 2020]

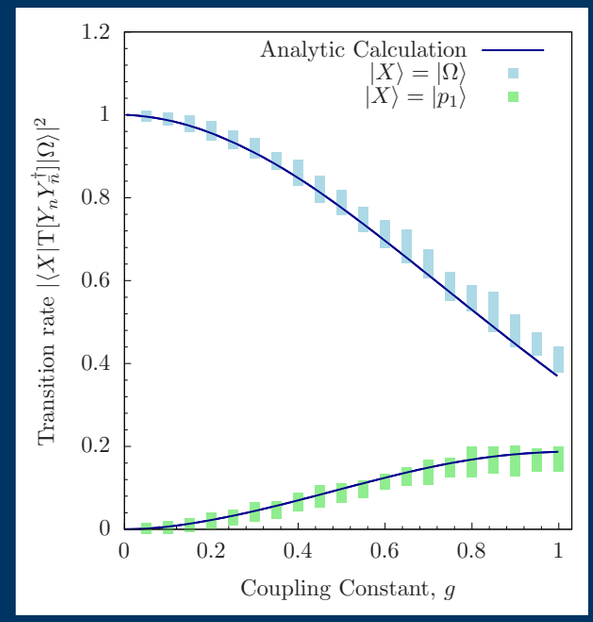

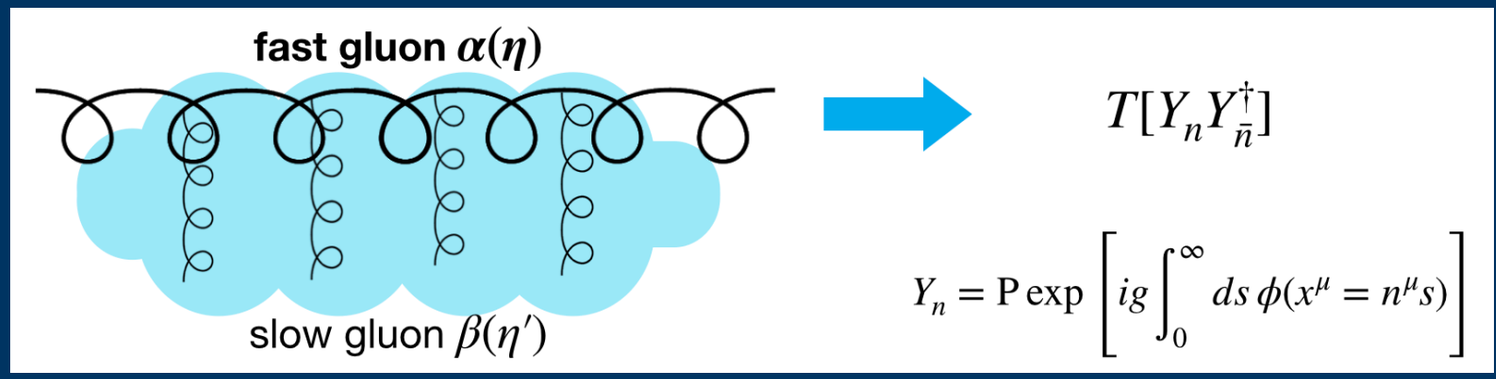

[C. W. Bauer et al., 2021] **Soft functions**

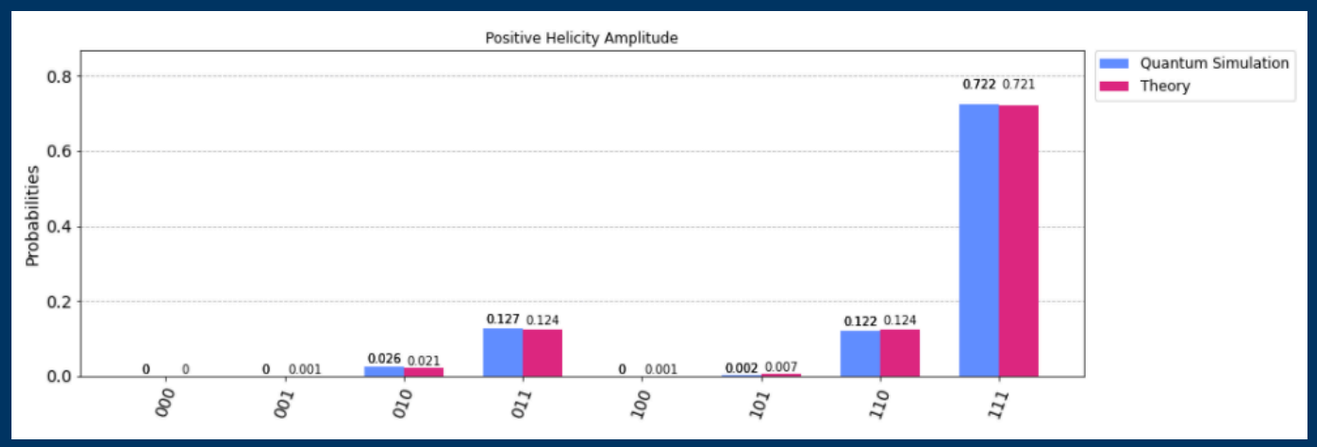

Hard scatterings

K. Bepari et al., 2020]

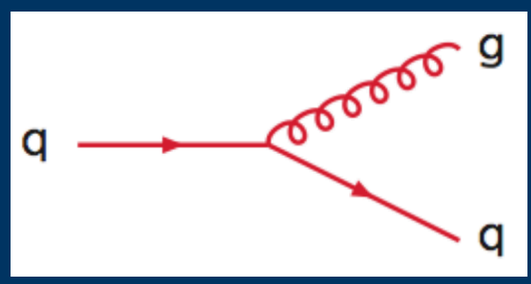

[T. Li et al., 2021]

PDFs

FFs